6-3-3-5

6-90-63-20 • 1 MAY 1963

TECHNICAL REPORT: PHYSICS

ON THE ORIGIN OF THE ANOMALOUS PHOTOVOLTAIC EFFECT IN ZINC SULFIDE

6-90-63-20 • 1 MAY 1963

6-90-63-20

TECHNICAL REPORT: PHYSICS

ON THE ORIGIN OF THE ANOMALOUS PHOTOVOLTAIC EFFECT IN ZINC SULFIDE

by

FRANK A. JUNGA

WORK CARRIED OUT AS PART OF THE LOCKHEED INDEPENDENT RESEARCH PROGRAM
AND ALSO SUPPORTED BY Nonr CONTRACT NO. 222(57)

Lockheed

MISSILES & SPACE COMPANY

A GROUP DIVISION OF LOCKHEED AIRCRAFT CORPORATION

SUNNYVALE, CALIFORNIA

NOTICE

QUALIFIED REQUESTERS MAY OBTAIN COPIES OF THIS REPORT FROM THE ARMED SERVICES TECHNICAL INFORMATION AGENCY (ASTIA). DEPARTMENT OF DEFENSE CONTRACTORS MUST BE ESTABLISHED FOR ASTIA SERVICES, OR HAVE THEIR NEED-TO-KNOW CERTIFIED BY THE MILITARY AGENCY COGNIZANT OF THEIR CONTRACT.

COPIES OF THIS REPORT MAY BE OBTAINED FROM THE OFFICE OF TECHNICAL SERVICES, DEPARTMENT OF COMMERCE, WASHINGTON 25, D.C.

DISTRIBUTION OF THIS REPORT TO OTHERS SHALL NOT BE CONSTRUED AS GRANTING OR IMPLYING A LICENSE TO MAKE, USE, OR SELL ANY INVENTION DESCRIBED HEREIN UPON WHICH A PATENT HAS BEEN GRANTED OR A PATENT APPLICATION FILED BY LOCKHEED AIRCRAFT CORPORATION. NO LIABILITY IS ASSUMED BY LOCKHEED AS TO INFRINGEMENT OF PATENTS OWNED BY OTHERS.

FOREWORD

This research was supported through the Lockheed Independent Research Fund, and by the University of California under Nonr Contract No. 222(57).

CONTENTS

ILLUSTRATIONS

I. INTRODUCTION

A. GENERAL FEATURES OF THE ANOMALOUS PHOTOVOLTAIC EFFECT

Certain crystals of ZnS generate voltages greater than the band gap voltage when illuminated with ultraviolet light. This phenomenon is called the anomalous photovoltaic effect.[1]

It is well known, from thermodynamic arguments,[2,3] that the maximum photovoltage a semiconductor device can generate is equal to its band gap voltage. Further studies by Merz[4] show that this photovoltage can be "quenched" by simultaneously illuminating the crystal with more than one wavelength of light. Cheroff and Keller[5] found that the polarity of the photovoltage is dependent on the wavelength of the incident light. Figure 1 is a graph of the open-circuit voltage and short-circuit current as a function of the wavelength of the incident light, for a typical crystal used in the present study.

In general, it is found that at wavelengths longer than 350 mμ, the photovoltages are of the order of 1 volt or less. At about 350 mμ the photovoltage reverses polarity and reaches a maximum at approximately 340 mμ . This maximum (to be called the positive peak) can be of the order of 100 volts. At shorter wavelengths (approximately 330 mμ) the photovoltage again changes polarity and increases to a maximum (of the opposite polarity). This negative peak is often of the same order of magnitude as the positive peak, but can be greater in absolute magnitude than the positive peak.

At still shorter wavelengths, the behavior varies. In some crystals, the photovoltage decreases to zero and in others the photovoltage persists to very short wavelengths (approximately 280 mμ).

Fig. 1 Spectral Dependence of Anomalous Photovoltaic Effect

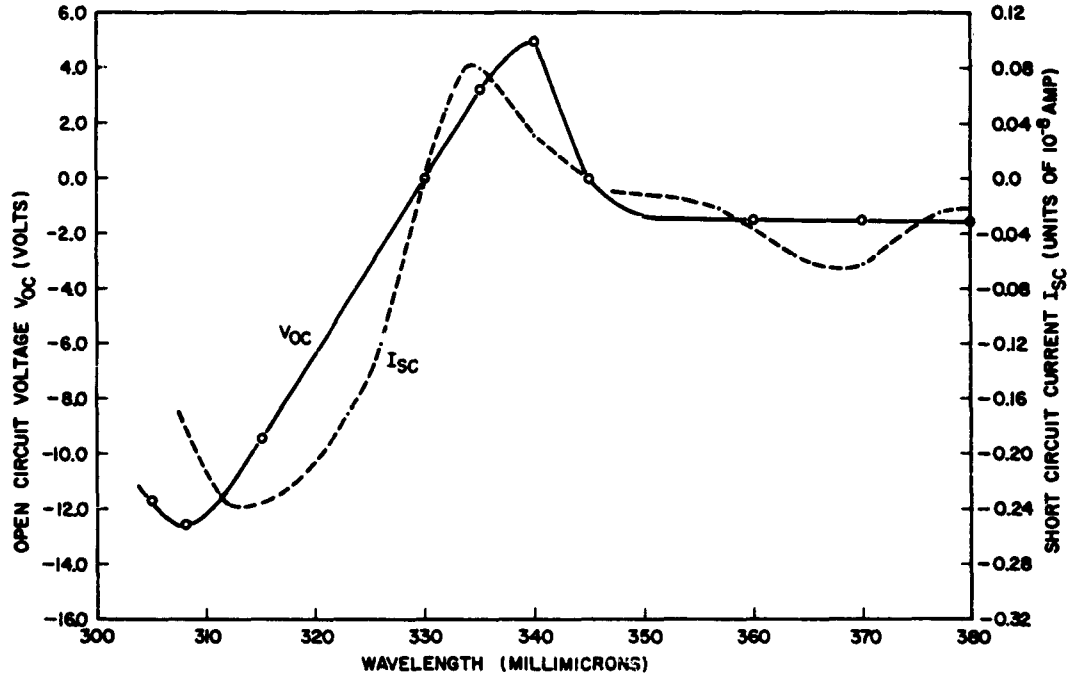

Typical spectral dependence of the open-circuit voltage V_{OC} and short-circuit current I_{SC} for a ZnS crystal exhibiting anomalous photovoltaic effect.

The purpose of this study will be to devise and justify a model (semi-quantitative) to account for the general features of the anomalous photovoltaic effect.

B. SOME PROPERTIES OF ZnS

Before reviewing more of the work done on the anomalous photovoltaic effect (APE), a survey of some of the properties of zinc sulfide will be helpful.

Zinc sulfide exists in both the cubic (sphalerite) and hexagonal (wurtzite) structures. Allen and Crenshaw[6] find that the cubic phase transforms into the hexagonal phase on heating to 1020°C. This figure for the transition temperature must be viewed with some reservation, since it has been found that the transition temperature is dependent on the purity of the sample used.[7] Allen and Crenshaw's work was done on a sphalerite specimen containing 0.15% Fe. The presence of chlorides either lowers the transition temperature or at least speeds the transition. Kremheller[7] finds no transformation even at temperatures as high as 1175°C in the absence of chlorine, a common contaminant in even the purest material. There is also some evidence[8,9] that the hexagonal phase transforms back to the cubic phase at 1240°C. One important feature of the transformation at 1020°C is that the transformation back to cubic from hexagonal on cooling from above 1020°C is extremely slow.[6] In fact, it is possible to cool the sample to room temperature without transformation into the cubic phase.

It is significant that only crystals grown from the vapor phase show anomalous behavior. This method generally produces needle-like crystals up to 1 cm long. The diameter of the crystals is usually a fraction of a millimeter. Structurally perfect crystals (either hexagonal or cubic) are rarely, if ever, produced by this method. Usually the crystals display some kind of stacking disorder.[8] The one

characteristic all crystals grown in this manner have in common is that the long axis of the crystal is either the cubic [111] axis or the hexagonal "c" axis.

Some information about the optical band edge of both phases of ZnS is essential to the analysis of the APE. Kröger[10] finds that cubic material displays a sharp edge at 340 $m\mu$. This result is confirmed by Beun and Goldsmith.[11] The results of measurements of the optical band edge of hexagonal material by various researchers are not in as good agreement as the measurements on cubic material. Piper and others[5, 12, 13, 14] find an edge at approximately 335 $m\mu$. However, Beun and Goldsmith[11] place the edge at approximately 330 $m\mu$. Since structurally pure crystals are rarely found, and the presence of any cubic material will shift the edge to longer wavelengths, it is felt that the results of Beun and Goldsmith are the most reliable. The effect of polarized light on the position of the band edge is also known and will be useful.[11, 14]

C. ESSENTIAL FEATURES OF THE APE

The most significant observation to come out of the early research[4] is the fact that only crystals displaying "banding" (when viewed between crossed polarizers) produce anomalous effects. Such crystals are thought to be composed of layers of hexagonal and cubic material.[15, 16] A. Lempicki[17] finds, by means of x ray analysis, that pure hexagonal crystals show no anomalies. On the evidence supplied by his own optical observations, Merz[4] proposes that the anomalously high photovoltages can be accounted for on a model which postulates the additivity of voltages generated by some simple, normally behaving unit. Thus, by counting the bands observed on crystals between crossed polarizers, Merz[4] estimates that the voltage due to one unit must be approximately 0.1 volt. Furthermore, if a crystal which displays uniform banding is broken in half, each part produces

approximately half the photovoltage observed for the whole crystal.* Merz's own model,[4] which does not account for the spectral response curve (it had not been measured at that time), cannot account for the high voltages since, as pointed out by Tauc,[18] it predicts zero photovoltage at high light levels. This is in contradiction to Merz's own data.

Another significant observation[4] is that high voltages are recorded only along the long ("c") axis of the crystal. This is confirmed by measurements on platelets of ZnS. For these crystals, the "c" axis can be determined optically. Merz also noted that there is a definite relation between the direction of growth and the polarity of the photovoltage (in his work, this is the positive peak photovoltage). Lempicki[17] finds no such correlation, but notes that the direction of the positive peak is correlated with the direction of the "c" axis as determined by pyroelectric measurements. In this experiment, Lempicki found that the end of the crystal which became positive on heating was positive at 340 mμ. All researchers[4, 5, 11, 17] find that the positive peak falls at a wavelength near the absorption edge previously reported for hexagonal ZnS.

*Lempicki[17], however, states that merely picking up a crystal with forceps can alter its characteristics. Thus, Merz's results on breaking crystals could be questioned.

II. EXPERIMENTAL PROCEDURE

A. SAMPLE PREPARATION

ZnS crystals can be grown by the sealed tube sublimation technique described by Reynolds and Czyzak.[13] RCA "Luminescent" grade ZnS powder, the purest commercially available, is the starting material. This powder is free from activators. The ZnS powder is placed in a clean, dry, quartz tube of the form shown in Fig. 2a. The tube is evacuated to a pressure of approximately 10^{-5} Torr and both the tube and ZnS powder outgassed by heating to about 900°C. The tube is then back-filled with about 10 Torr of H_2S, sealed off and placed in a tubular furnace possessing a temperature gradient. The charge of ZnS is placed in the hottest region of the furnace and the temperature there maintained at about 1170°C. At this temperature, the vapor pressure of ZnS is nearly 10 Torr (Ref. 19). The ZnS vapor condenses on the coolest surfaces of the tube, and, under the proper conditions, crystals are formed at about 1000° C. It normally takes 120 hours to produce crystals of usable dimensions. The role played by the H_2S is not known, but it does not act as a chemical transport gas as does iodine in the work of Nitsche,[20] since the material transport rate decreases with increasing H_2S pressure.

The peculiar shape of the receiving surfaces (Fig. 2a) enhances crystal growth. Attempts to grow crystals in tubes without the short inner tube (Fig. 2b) are much less successful. Instead of obtaining single crystals, a heavy layer of polycrystalline material is deposited on surface C. In the type of tube shown in Fig. 2a, crystals appear on surface A, and a thin polycrystalline layer forms on surface B. Surfaces B and C are cooler than surface A, since the former

Fig. 2 Crystal Growing Tubes

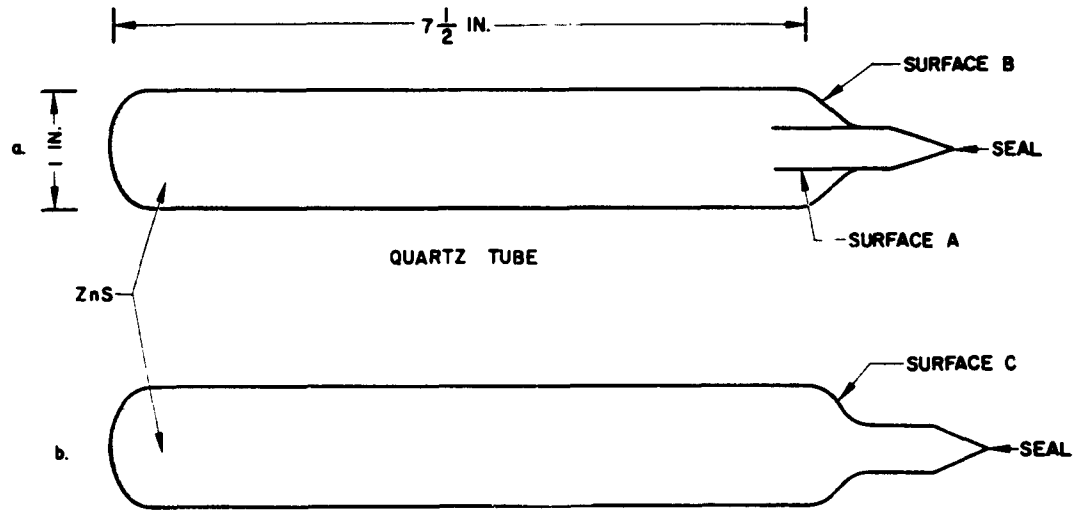

Typical tubes used in the sublimation method of growing ZnS crystals. Tubes of type "a" produced better crystals.

"see" the cold end of the furnace and can be cooled by radiation. Surface A radiates radially toward the 1000°C inner surface of the furnace. The fact that surfaces B and C are cool decreases the allowable vapor pressure locally, thus enhancing the chance of growth. The fact that surface A is warmer favors the growth of single crystals.

B. MEASUREMENTS

The principal measurement made in this study was the spectral response of the anomalous photovoltaic effect. This measurement was made at varying light levels and on both stressed and unstressed crystals. Other auxiliary measurements (photoconductive effect and piezoelectric effect) will be helpful in devising the model.

1. Optical Apparatus

The essential elements in the experimental equipment are a source of monochromatic light, and an electrometer. A Leiss single-pass, quartz prism, monochromator in conjunction with a high-pressure, water-cooled mercury arc provides the monochromatic light. The lamp is rated at approximately 1000 watts. However, it is not a continuous source. The lines are pressure broadened so that there is a continuous background, but there still are some large peaks in the output of the lamp. As equipment is not available to calibrate the lamp absolutely, the curves of spectral response depicted in the present study are uncorrected for variations in light intensity.

The monochromator dial setting (which determines the output wavelength) can be calibrated by using a standard spectral lamp as a line source, and comparing the observed spectrum with a map of the spectrum (e.g., Eder: Atlas Typischer

Spektren). Variations in intensity of the light incident on the sample are accomplished by placing copper screens in the light beam.

As the impedance of these ZnS crystals is often of the order of 10^{12} ohms, it is necessary to use an electrometer to measure the photovoltage. The electrometer (Keithly 200B) has an input impedance of approximately 5×10^{14} ohms. The short-circuit current is observed by measuring the voltage drop across a calibrated shunt resistor. The shunt resistance must be considerably lower than the sample resistance.

2. Electrical Contacts and Connections

Electrical contact to ZnS can be made with silver paint. These contacts give the same results as Hg-In-Tℓ liquid contacts, and In-Hg alloy solder contacts. The silver paint contacts are the easiest to apply and were used on almost all of the samples.

A metal box, with accessories such as the sample holder (Fig. 3, 4) can be connected directly to the electrometer by means of bayonet-type plugs. This eliminates all leads outside the chassis.

3. Stress Measurements

Measurements of the spectral response of the photovoltaic effect on stressed crystals and measurement of the piezoelectric constant "g" are made with the same apparatus. Again the apparatus is built into a chassis which is connected directly to the electrometer. The stressing apparatus is shown in Fig. 5 and is self-explanatory. Silver paint is applied to the crystal and the crystal placed, end on, on the stainless steel pedestal. The set screw is then adjusted until contact is made with terminal A. A known mass is then lowered onto the phosphor bronze strip A' and the desired measurement is made.

Fig. 3 Crystal Support

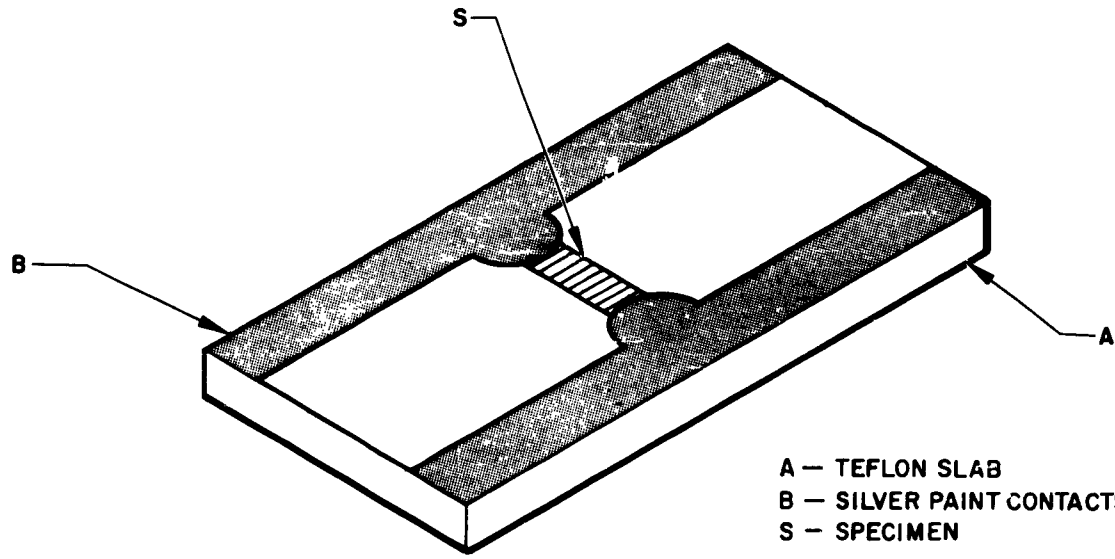

Crystals were mounted in this manner for measurements of photovoltaic effects, current-voltage characteristics, and photoconductance.

Fig. 4 Crystal Support Holder

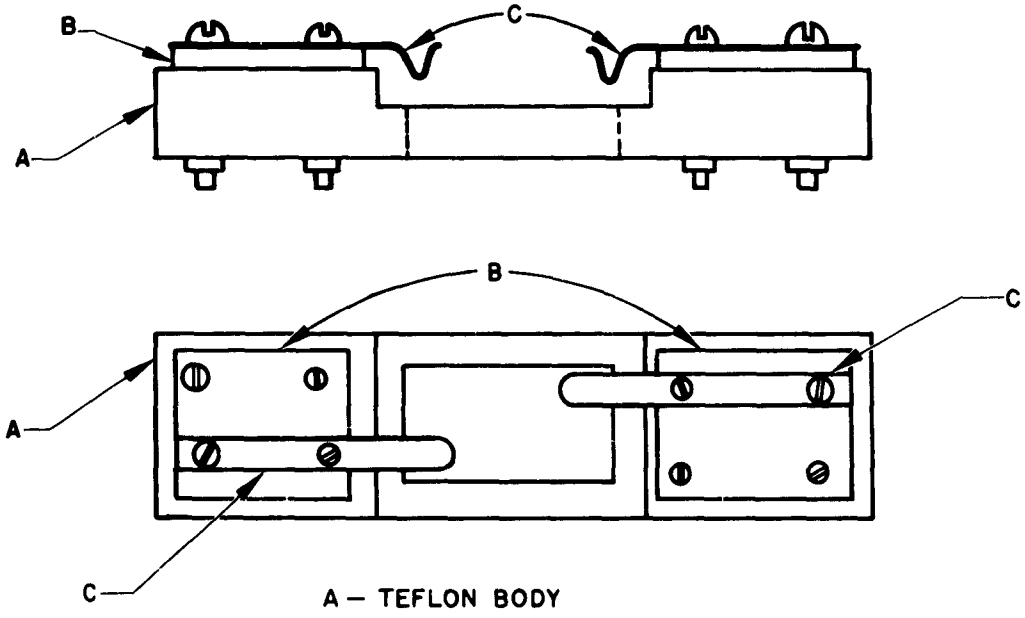

Fig. 5 Stress Apparatus (Longitudinal Section)

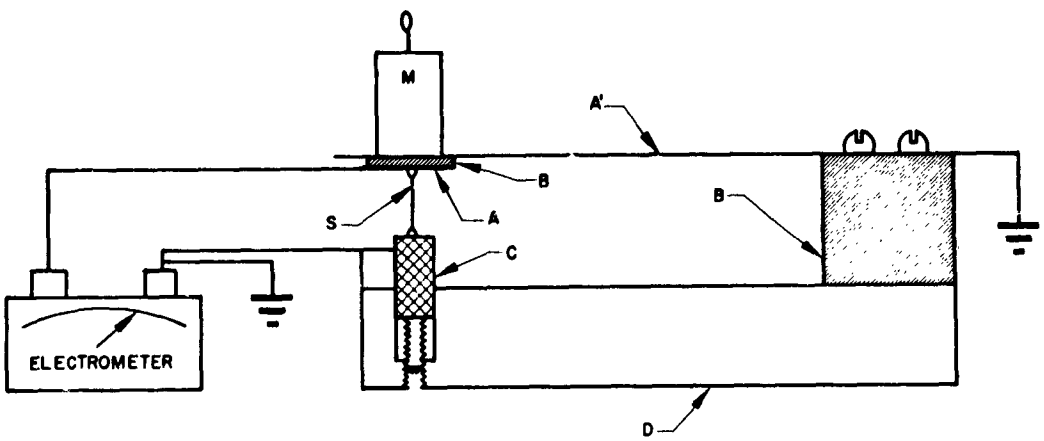

A,A' — PHOSPHOR BRONZE
B — TEFLON
C — STAINLESS STEEL PEDESTAL
D — BRASS BASE
M — WEIGHT
S — SPECIMEN

Schematic drawing of apparatus used to apply stress to crystals in measurements of the stress dependence of the anomalous photovoltaic effect and the peizoelectric constant "g."

4. Measurement of Current-Voltage Characteristics and Photoconductance

Both the current-voltage and photoconductance data are taken with the same circuit (Fig. 6). It should be noted that R_S must be kept approximately two orders of magnitude lower than the sample resistance. R_B is always at least an order of magnitude lower than R_S.

Fig. 6 Measuring Circuit

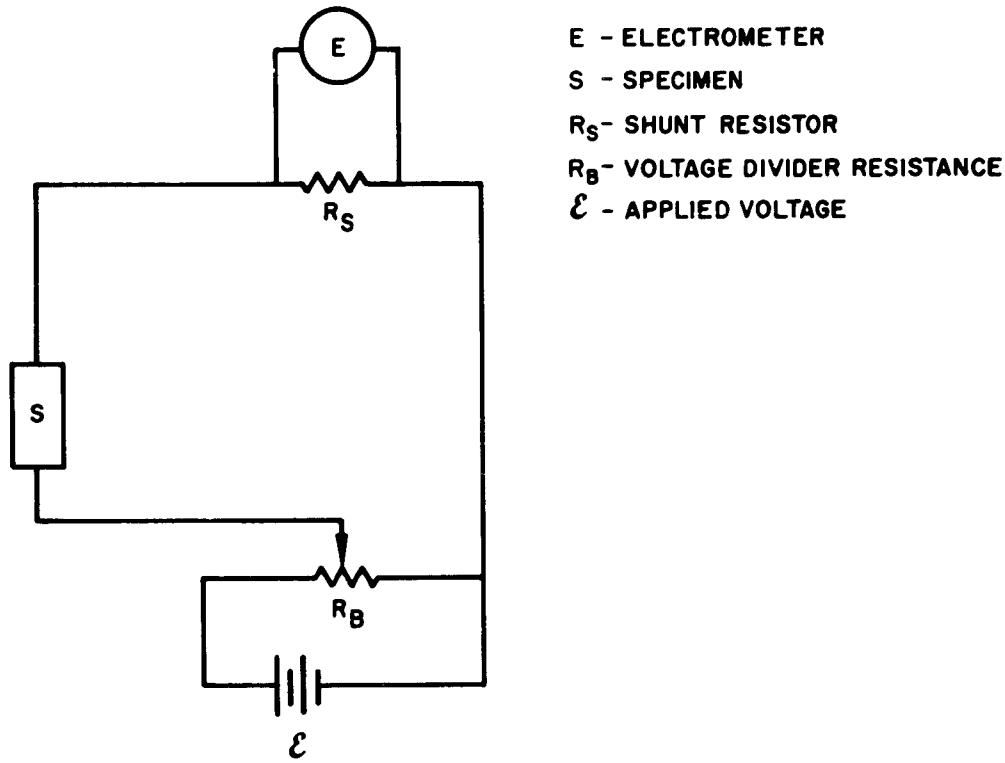

Circuit used to measure current-voltage characteristics and photoconductance of ZnS crystals.

III. PROPOSED ORIGINS OF ANOMALOUS PHOTOVOLTAIC EFFECT

A. REVIEW AND CRITICISM OF PROPOSED MODELS

Two postulates are common to the three models proposed to account for the anomalous photovoltaic effect in ZnS: First, both hexagonal and cubic material must be present in the crystals in alternating layers (perpendicular to the "c" axis); second, the observed high voltage is the sum of voltages generated in each layer or between layers (called segments).

Tauc's model[18] makes use of the fact that there is about a 0.1 ev difference in band gaps between the hexagonal and cubic phase of ZnS (3.75 ev and 3.65 ev, respectively[11]). Tauc also assumes that an impurity gradient (donor or acceptor) exists in each segment. Tauc shows[21,22] that changes in band gap and impurity gradients can produce photovoltages. The model is so constructed that the impurity gradient photovoltages (bulk photovoltages) are opposed to the photovoltage generated by the differences in band gap. The spectral response of the APE can be accounted for on this model because of the nature of the band gap photovoltage. This voltage is generated only when both the hexagonal and cubic phases are absorbing.

On the other hand, the bulk photovoltages depend only on the absorption in their respective phases. Thus, at long wavelengths (e.g., 400 mμ) a bulk photovoltage in the cubic phase is generated. For an impurity gradient which changes the resistivity of the material by 50% over the length of the segment, this voltage will be about 1.0×10^{-3} volts.[22] As the wavelength is decreased to a point where the hexagonal phase absorbs, the band gap photovoltage is generated, and for still shorter wavelengths, the hexagonal phase becomes very absorbing and a bulk photovoltage in that phase is generated. Since the bulk and band gap voltages

are opposed, there will be a wavelength at which the band gap photovoltage (0.1 ev) counteracts the cubic bulk photovoltage and the resultant voltage is zero. The band gap photovoltage then increases and reaches a maximum. The maximum observed photovoltage is the band gap photovoltage reduced by the two bulk photovoltages.

In order for the polarity of the photovoltage to change again, Tauc assumed that the band gap photovoltage decreases sharply at about 330 mμ. He proposes that the electrons excited at this wavelength have sufficient energy to tunnel through the barrier. At very short wavelengths (e.g., < 330 mμ) the observed photovoltage is due to the two bulk photovoltages. The high voltage observed at the positive peak is then the sum of the band gap voltage generated between each layer.

This model has one obvious drawback. Essentially, the high positive peak photovoltage is due to the 0.1 volt generated at each band gap change (this is the maximum voltage one can generate from this configuration[22, Sect. 4.2]). Since this voltage is due to the change in band gap, it is not reversible in the sense that it also could account for the high voltages at the negative peak. Another drawback of this model is the method of addition of photovoltages. To examine this facet of the model, consider the following band diagram for a region of a segmented crystal.

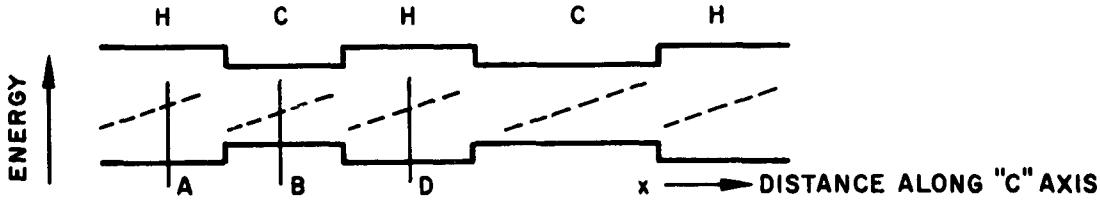

The broken lines represent the impurity gradients. At first glance it appears that the photovoltage V_{AB} would be exactly counteracted by V_{BD}, and that no addition could take place. However, since the impurity density changes along a segment, $\Delta\sigma/\sigma$ (the relative change in conductivity under illumination) is also a function of x and the combination of change in band gap and change in $\Delta\sigma/\sigma$ allows one to add the voltages (see Sect. III-C) at each band gap change. Unfortunately, in order to obtain the full band gap voltage, $\Delta\sigma/\sigma$ must vary considerably along the segment. In fact, for a 50% change in conductivity along each segment (about what is necessary to generate the long wavelength negative voltage), a photovoltage of only $(0.3\ \Delta Eg)/e$ can be realized between points A and D – not nearly enough to support Merz's data.

G. Neumark[23] has proposed a model which also uses the band gap voltage as the origin of the anomalously high positive peak photovoltage. Again, this model cannot account for the high negative peak photovoltage. Addition of the individual band gap voltages is taken care of by modulating the conductivity by means of internal polarization fields.

Thus, both these models break down for the same reason. It appears that any model based on the band gap photovoltage cannot account for all aspects of the APE.

The final model to be discussed was proposed by A. R. Hutson.[24] This model makes use of the fact that both phases of ZnS are piezoelectric* and that the transverse lattice constant of the hexagonal phase is smaller than the cubic lattice constant.

*Cubic ZnS is piezoelectric only in shear, which is all that is needed in this case.

In brief, Hutson proposes that when there is a crystal phase transformation during the growth process, a transverse strain is frozen into the crystal. The material on the hexagonal side of the transition is in tension and the material on the cubic side is in compression (see Fig. 7). Since ZnS is piezoelectric, there will be fields generated within each segment. In the dark, these fields are compensated for by fields set up by the diffusion of carriers, as is the case in any solid state photovoltaic device.[22] Under illumination, however, these fields can give rise to a photovoltage. Hutson proposes that the spectral response be accounted for in some way with the difference in absorption coefficients between the two phases. Hutson's presentation is descriptive and he makes no attempt to calculate the photovoltage on the basis of his model. He is also not specific on how the photovoltages add. In the following sections, Hutson's model will be extended to show how the spectral response curve can be accounted for. In addition, an expression for the photovoltage generated by a strained crystal will be calculated and a model set up to show how the photovoltages in each segment add.

B. EXTENSION OF HUTSON'S MODEL

1. Discussion

The data to be presented later will be used to justify a model based on Hutson's ideas. Before presenting the data, this extended model will be considered in detail.

This model is predicated on two assumptions:

(1) Strains exist at the transition between the hexagonal and cubic segments.
(2) The hexagonal segments are slightly more absorbing than the cubic segments at wavelengths of 400 mμ and longer.

Fig. 7 Variation of Lattice Constant in Vicinity of Structure Change

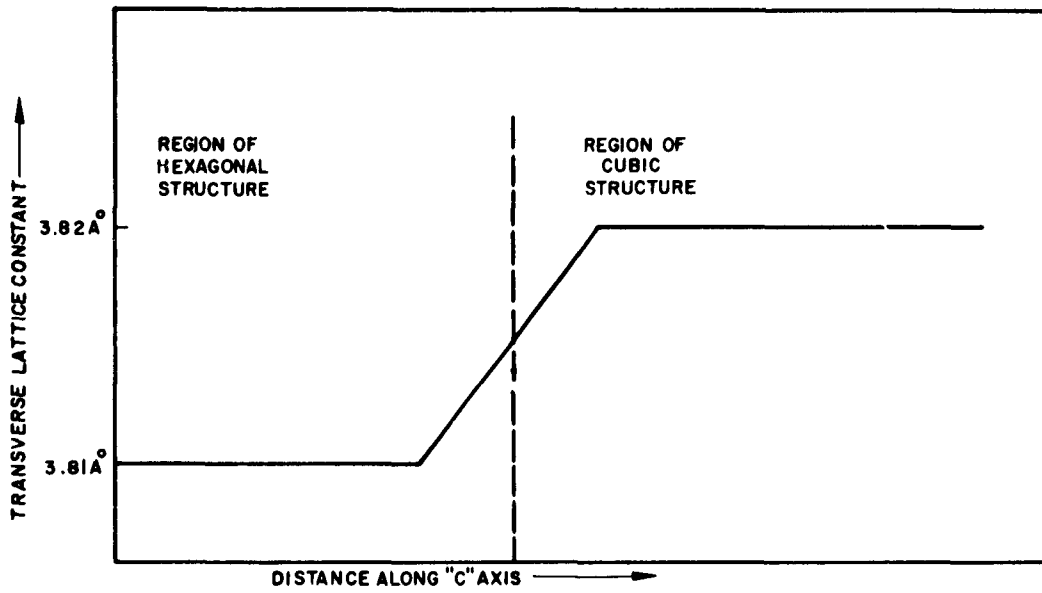

Schematic variation of transverse lattice constant along "c" axis of a mixed structure ZnS crystal, in the vicinity of a structural change. This is the type of variation used in the calculation of the photovoltage for the extended Hutson model.

For simplicity, the crystal will be considered as composed of one layer each of cubic and hexagonal material. Then, by Assumption (1) and the discussion in the previous section, opposing fields can exist in the two segments. It is these fields which, when non-equilibrium electron-hole pairs are created by light, give rise to the photovoltages. The magnitude of these photovoltages is dependent on the number of electron-hole pairs created (see Sect. III-B.3) and thus on the absorption coefficients of the material (Fig. 8). Since by Assumption (2), hexagonal material absorbs more at long wavelengths, a small voltage will be generated by the field in the hexagonal segment. This voltage is chosen as negative and is observed at wavelengths longer than 350 mμ. As the wavelength is decreased, the absorption edge of the cubic phase is approached, and the cubic phase begins to absorb. The field in this phase produces a photovoltage which counteracts the long wavelength voltage. The resultant voltage then goes to zero ($\sim$348 mμ). This wavelength is very close to the region where the absorption coefficient of cubic ZnS increases. As the cubic material absorbs more heavily, its photovoltage increases. This photovoltage (denoted the positive peak) reaches its maximum at $\sim$340 mμ (the cubic band edge[11]), then begins to decrease.*

In the region between 330 and 335 mμ, hexagonal ZnS begins to absorb. The resultant increase in the voltage in this segment counteracts the positive peak voltage and is the cause of the decrease in observed photovoltage in this region. Eventually the voltage generated by the hexagonal segment exactly counteracts the voltage in the cubic segment and the observed photovoltage is zero ($\sim$330 mμ). At shorter wavelengths it is maintained that the absorption coefficient of cubic

*The fact that the short-circuit current peaks at 335 mμ is due to a bright line in the Hg source.

Fig. 8 Wavelength Dependence of Transmission of Hexagonal and Cubic ZnS

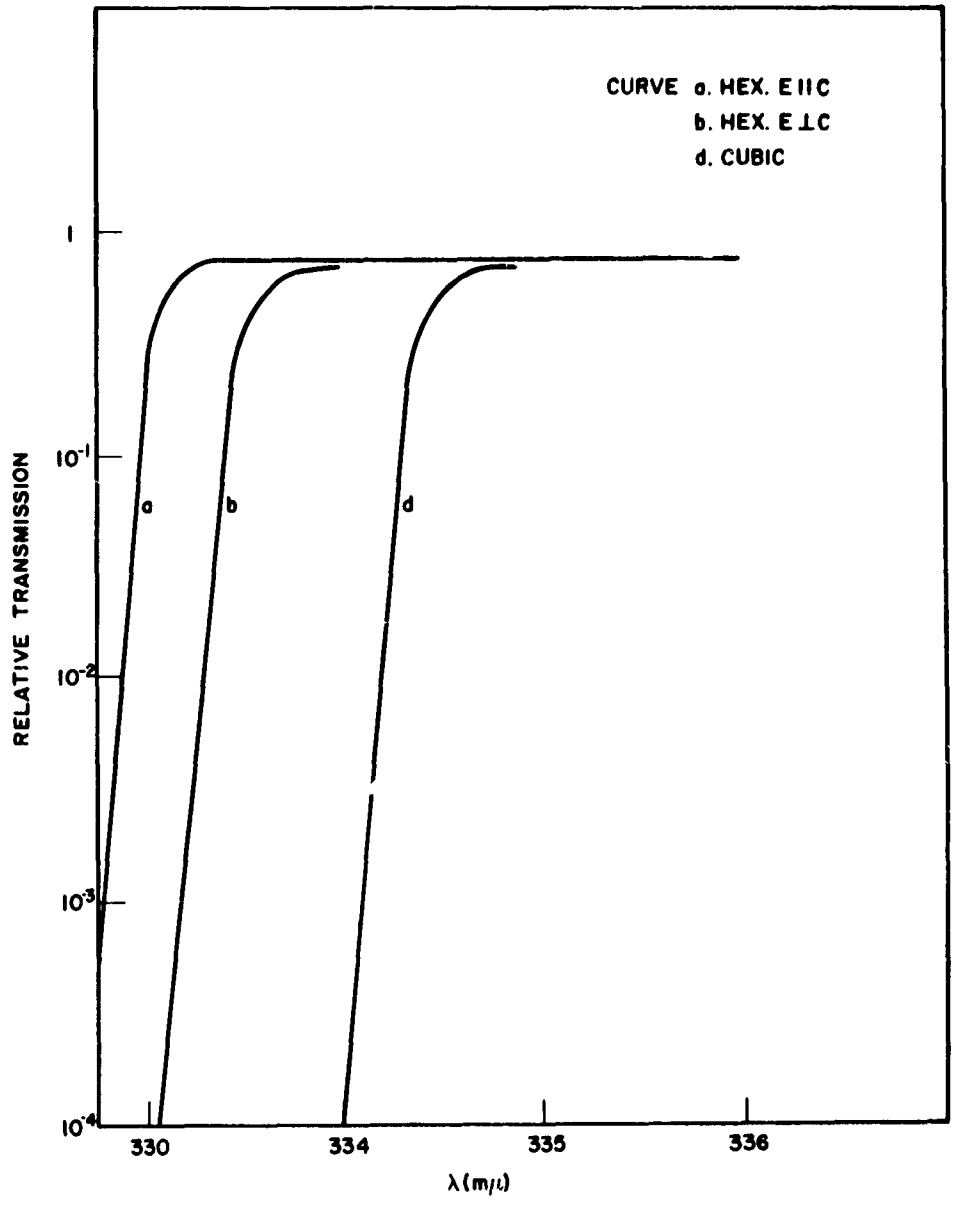

Change in optical transmission in the vicinity of the band edges of hexagonal and cubic ZnS. Curve "a" is for hexagonal material with the electric vector E of the incident light parallel to the "c" axis, curve "b" is for E⊥ (c), and curve "d" is for cubic material [after Beun and Goldsmith, Helv. Phys. Acta 33, 508 (1960)].

ZnS is so large that carriers are only created on the surface and do not participate in the photovoltaic effect. As the wavelength is decreased, the photovoltage generated by the hexagonal segment reaches its maximum (the negative peak). At still shorter wavelengths, the absorption coefficients of both phases are so high that no carriers are generated in the bulk of either phase and the photovoltage decreases to zero.

This argument can account for the spectral response of the APE. In order to produce the high voltages observed at the positive and negative peaks, note that in these two regions the voltage is associated with one or the other phase, not both. That is, at the positive peak, virtually only cubic material absorbs; at the negative peak, only the hexagonal phase absorbs (absorbing in the sense of producing electron-hole pairs in the bulk of the crystal). Thus, when conditions are right for a peak, the crystal as a whole is composed of alternating segments of absorbing and non-absorbing layers. This configuration allows the voltages of the absorbing segments to add (see Sect. III-C).

One serious objection against the model as presented here is the matter of symmetry of strains in the crystal. That is, since the crystal is composed of alternating layers of hexagonal and cubic material, is not the contribution to the photovoltage of the strains at a cubic to hexagonal transition exactly counteracted by the contribution from a hexagonal to cubic transition? Fortunately, this is not the case. As pointed out by Allen and Crenshaw,[6] the hexagonal to cubic transition is very sluggish, so that the strain may be spread over a much larger distance along the crystal at the hexagonal to cubic transition. This sluggishness may also allow impurities to migrate to this transition region and release the strain. Furthermore, as will be seen in the next section, the photovoltage depends on the strain gradient rather than the strain. Thus, it is possible for

the cubic $\rightleftharpoons$ hexagonal transitions to be asymmetric (as far as the photovoltaic effect is concerned).

2. Extension of Hutson's Model – Derivation of Photovoltage

a. Method. The photovoltage generated by a nonuniformly strained piezoelectric crystal will be derived for a one-dimensional crystal in which the strain falls off linearly with distance and is zero for most of the crystal (Fig. 9). This photovoltage will be associated with one of the segments of a ZnS crystal. Similar expressions apply to the other segments and the observed photovoltage will be obtained by addition of these elemental voltages. The program of the derivation is as follows:

(1) The electrostatic potential V inside the crystal will be calculated.

(2) Since the electrochemical potential μ is a constant throughout the segment,[25] the slope of the chemical potential $d\zeta/dx$ can be found from step (1) and the relations $\mu = \zeta - eV$ and $d\mu = 0$.

(3) $d\zeta/dx$ will be expressed in terms of dn/dx, the slope of the carrier concentration along the crystal.

(4) Finally, dn/dx will be used to calculate the photovoltage.[21, 22]

b. Calculation of the Electrostatic Potential V. The relation between field E, displacement D, dielectric constant ϵ, piezoelectric constant g, and stress Π is given by Mason:[26]

$$E = \frac{D}{\epsilon} - g\Pi \qquad (1)$$

Π is related to the strain S by the relation

$$\Pi = Ss \ ,$$

Fig. 9 Variation of Strain Along Crystal Segment

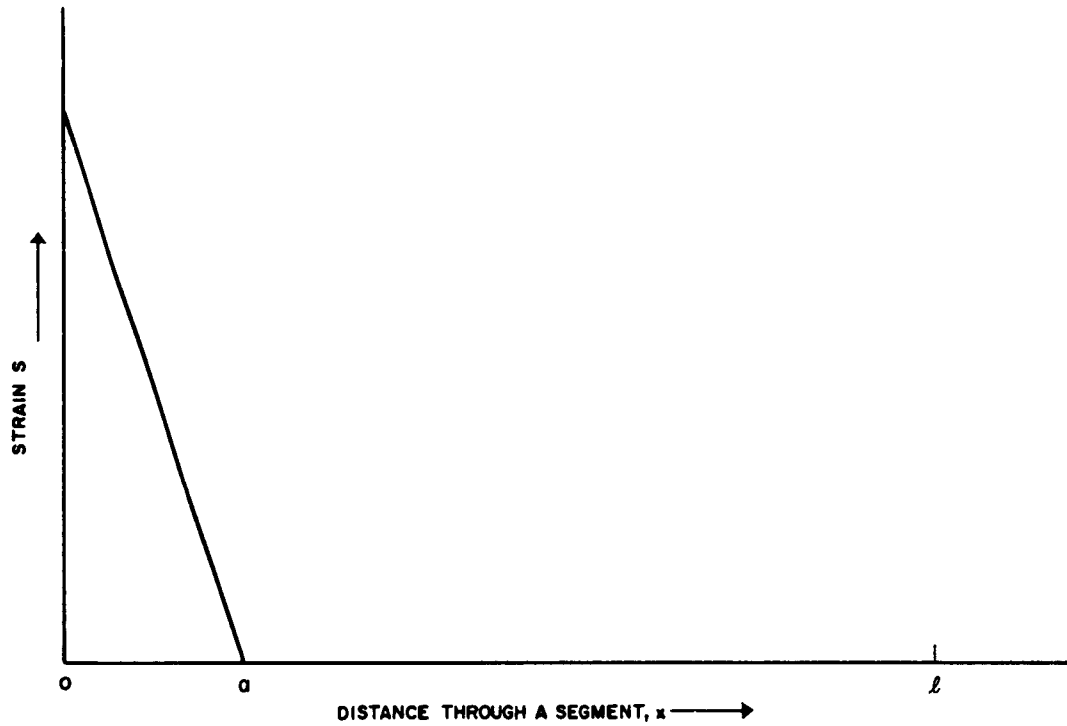

Proposed variation of transverse strain S with distance along "c" axis of a mixed crystal of ZnS. This configuration was used in the calculation of the photovoltage in the extended Hutson model.

where s is a constant (the elastic stiffness). Thus, Poisson's equation becomes

$$\epsilon \frac{dE}{dx} + \epsilon g s \frac{dS}{dx} = 4\pi\rho \ , \tag{2}$$

where ρ is the net charge density. For an n-type semiconductor with carrier concentration n and N fully ionized donors per unit volume,[27]

$$\rho = -e(n - N) \ ,$$

and Equation (2) can be rewritten as

$$-\frac{d^2V}{dx^2} = -gs\frac{dS}{dx} - \frac{4\pi e}{\epsilon}(n - N) \ . \tag{3}$$

Furthermore, n is related to ζ by

$$n = N_c \exp\left[\zeta/kT\right] \ , \tag{4}$$

where N_c is the effective density of states in the conduction band. Demanding that electrical neutrality be maintained far from the strain and that V is zero far from the strain, i.e. ,

$$n \to N \quad \text{and} \quad V \to 0 \quad \text{as} \quad x \to \infty \ ,$$

then using the relation between ζ and μ,

$$N = N_c \exp\left[\mu/kT\right] \ .$$

Therefore, Equation (4) can be rewritten as

$$n - N = N_c \exp\left[\mu/kT\right] \left\{\exp\left(eV/kT\right) - 1\right\}$$

or,

$$n - N = n_o \left\{\exp\left(eV/kT\right) - 1\right\} \quad , \tag{5}$$

where n_o is the carrier concentration in the absence of strain. Then combining Equations (3) and (5),

$$\frac{d^2V}{dx^2} = g s \frac{dS}{dx} + \frac{4\pi e n_o}{\epsilon} \left\{\exp\left(eV/kT\right) - 1\right\} \quad . \tag{6}$$

For the sake of simplicity, S is chosen as

$$S = \alpha \left(1 - \frac{x}{a}\right) \quad ,$$

where α is the strain at the interface. Thus, Equation (6) becomes

$$\frac{d^2V}{dx^2} = - g s \frac{\alpha}{a} + \frac{4\pi e n_o}{\epsilon} \left\{\exp\left[eV/kT\right] - 1\right\} \quad . \tag{7}$$

For calculation, the potential is divided into two parts: V_1 valid for $0 < x < a$ and V_2 valid for $a < x < \ell$. The boundary conditions are

$$V_1 = V_2 \quad \text{and} \quad \frac{dV_1}{dx} = \frac{dV_2}{dx} \quad \text{at } x = a,$$

$$V_2 = \frac{dV_2}{dx} = 0 \quad \text{for } x \to \ell \quad .$$

Under these conditions, and assuming V_2 is small,

$$V_2 = V_o \exp\left[-\sqrt{\frac{we}{kT}}\ x\right] \quad , \tag{8}$$

where $w = 4\pi e n_o/\epsilon$ and V_o is an integration constant. In the region $0 < x < a$, in order to obtain a solution in closed form, it is necessary to consider the strain term dominant.* With this restriction, V_1 becomes

$$V_1 = \frac{\beta x^2}{2} + \gamma\, x + \delta \quad , \tag{9}$$

where $\beta = -(gs\alpha)/a$ and γ and δ are integration constants. Evaluating the constants of integration, one finds

$$V_o = \left(\beta\, a^2/2\right)\left[e^{-ta}\,(1 + ta)\right]^{-1} ,$$

$$\gamma = -\beta\, a\,(3at + 2)\,\left[2(1 + ta)\right]^{-1} ,$$

$$\delta = \beta\, a^2 ,$$

$$t = (we/kT)^{1/2} .$$

3. Calculation of the Photovoltage

Tauc[21,22] has derived a rather general expression for the photovoltaic effect. This expression is used as a starting point for the photovoltage calculation. Tauc finds that the photovoltage U generated by an n-type semiconductor is given by:

*A consequence of this limitation is that this model will not be valid at very high light levels.

$$U = -\frac{kT}{e}\left\{\int\frac{\Delta\sigma}{\sigma+\Delta\sigma}\,\frac{1}{n}\frac{dn}{dx}\,dx + \frac{\mu_n-\mu_p}{\mu_n+\mu_p}\int\frac{d\Delta\sigma}{\sigma+\Delta\sigma}\right\} \tag{10}$$

where n is the carrier concentration, σ the conductivity, $\Delta\sigma$ the change in conductivity with illumination, and μ_n and μ_p are the electron and hole mobilities, respectively. The connection between the internal electrostatic potential V and the quantities in Equation (10) is made by means of the following relations

$$\left.\begin{aligned}\mu &= \zeta - eV\\ d\mu &= 0\\ n &= N_c e^{\zeta/kT}\end{aligned}\right\}. \tag{11}$$

From these equations, the relation between n and V is found:

$$\frac{1}{n}\frac{dn}{dx} = \frac{e}{kT}\frac{dV}{dx} \quad . \tag{12}$$

For convenience, make the following abbreviations,

$$\Theta = e/kT \qquad P = dV/dx \quad ,$$

and define $\Gamma(x)$ by

$$\Gamma(x) = \int \Theta P\,dx \quad . \tag{13}$$

Then Equation (12) becomes

$$\frac{1}{n}\frac{dn}{dx} = \frac{d\Gamma}{dx} \quad , \tag{13a}$$

and

$$\ln n = \Gamma(x) + \text{constant} \quad .$$

Thus, for the region $a < x < \ell$, with V_2 calculated in Section B, n becomes

$$n = n_o \exp\left[\left(eV_o/kT\right)e^{-mx}\right] = n_o e^{\Gamma_2(x)}, \tag{14}$$

where $m = \sqrt{\frac{we}{kT}}$.

Similarly, for the region $0 < x < a$, n becomes

$$n = n_o \exp\left[\left(e/kT\right)\left(\beta x^2/2 + \gamma x + \beta a^2\right)\right] - n_o e^{\Gamma_1(x)} \tag{15}$$

Using Equations (13a), (14) and (15), the first term in Equation (10) can be rewritten

$$\frac{-kT}{e}\int_o^{\ell} \frac{\Delta\sigma/\sigma_o}{e^{\Gamma} + \Delta\sigma/\sigma_o}\, d\Gamma \quad .$$

where $\sigma_o = n_o e\mu_n$. This integral is called the chemical voltage U_c.

Substituting for Γ_1 and Γ_2 and integrating

$$U_c = \frac{-kT}{e}\left\{\ln \frac{\frac{\Delta\sigma}{\sigma_o} e^{-\Gamma_1(0)} + 1}{\frac{\Delta\sigma}{\sigma_o} + 1}\right\} \quad . \tag{16}$$

The second term in Equation (10) is called the diffusion voltage U_d and is sometimes associated with the Dember Effect. This term gives the contribution to the photovoltage due to any difference in the mobilities of the carriers diffusing out of the illuminated region. Assuming that the density of excess carriers falls off linearly with distance outside the illuminated area one finds

$$U_d = \frac{-kT}{e} \frac{\mu_n - \mu_p}{\mu_n + \mu_p} \ln \left(\frac{1 + \frac{\Delta\sigma_o}{\sigma(1)}}{1 + \frac{\Delta\sigma_o}{\sigma(o)}} \right) ,$$

where the illuminated region extends from 0 to 1 and $\Delta\sigma_o$ is the change in conductivity with illumination between 0 and 1. From Equations (14) and (15) $\sigma(0)$ and $\sigma(1)$ can be found in terms of Γ_1 and Γ_2. Thus,

$$U_d = \frac{kT}{e} \frac{\mu_n - \mu_p}{\mu_n + \mu_p} \ln \left\{ \frac{1 + \frac{\Delta\sigma_o}{\sigma_o}}{1 + \frac{\Delta\sigma_o}{\sigma_o} e^{-\Gamma_1(0)}} \right\} . \tag{17}$$

Combining Equations (16) and (17), the total photovoltage U becomes

$$U = \frac{kT}{e} \left(\frac{2}{1 + 1/b} \right) \ln \left\{ \frac{1 + \frac{\Delta\sigma_o}{\sigma_o}}{1 + \frac{\Delta\sigma_o}{\sigma_o} e^{-\Gamma_1(0)}} \right\} , \tag{18}$$

where b is the ratio of electron-to-hole mobility and

$$\Gamma_1(0) = \frac{e}{kT} \beta a^2 .$$

As noted earlier, $\beta = -(gs\alpha)/a$ where $-\alpha/a$ is the slope of the strain. Thus, for a linear slope (with point "a" fixed)

$$\beta a^2 = gsa^2 \frac{dS}{dx} . \tag{19}$$

Equation (18) with (19) will be used to express the photovoltage developed in a single segment of the crystal.*

*Actually similar relations can be found for any strain function for which $\frac{dS}{dx} \neq 0$ at $x = 0$.

C. THE ADDITION OF ELEMENTAL PHOTOVOLTAGES

Consider the configuration below, which represents a ZnS crystal composed of three segments.

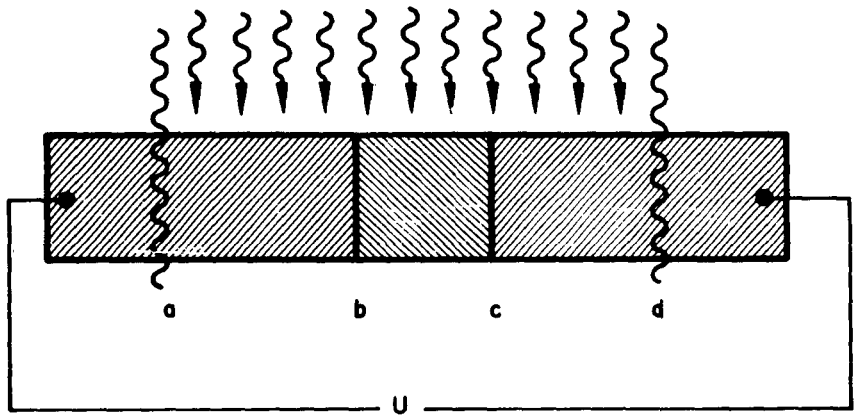

The two end regions are identical and the region b c has slightly different properties and the crystal is uniformily illuminated from a to d. The conduction band edge in the dark of such a configuration might be represented by the following picture.

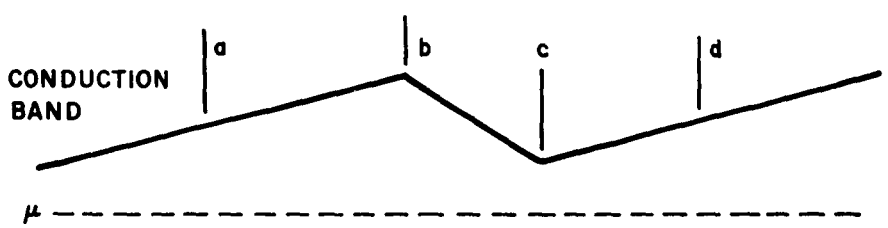

In the limit of very high light levels it appears that the voltage generated between a and b will be cancelled out by the voltage generated between b and c, since in this limit the photovoltage depends only on the difference in Fermi level (chemical potential ζ) between parts a and c. In this case, there can be no addition of

photovoltages (unless, of course, b c is a metal). However, at lower light levels, it will be shown that there can be addition of photovoltages. Qualitatively, one notes from Equation (18) that the photovoltage saturates at very high light levels. Thus, in order to get addition it is necessary for the photovoltage in b c to be unsaturated. Quantitatively, one can express the photovoltage U[22] as

$$U = \frac{-kT}{e} \frac{2}{1 + b} \int \Delta\sigma \frac{d\rho_o}{dx} dx \quad ,$$

where ρ_o is the dark resistivity and is a function of x. Since the first and third layers are identical, the following relations hold:

$$\Delta\sigma = \Delta\sigma_1 \qquad a < x < b$$

$$\Delta\sigma = \Delta\sigma_2 \qquad b < x < c$$

$$\Delta\sigma = \Delta\sigma_1 \qquad c < x < d \quad .$$

For convenience, assume that b is constant. Then U becomes

$$U = \frac{-kT}{e} \frac{2}{1 + b} \left\{ \Delta\sigma_1 \left[\rho_o(b) - \rho_o(a) + \rho_o(d) - \rho_o(c) \right] + \Delta\sigma_2 \left[\rho_o(c) - \rho_o(b) \right] \right\} .$$

But from the symmetry of the configuration,

$$\rho_o(a) = \rho_o(c); \quad \rho_o(b) = \rho_o(d) \quad ,$$

and U becomes

$$U = \frac{-kT}{e} \frac{2}{1 + b} \left\{ 2\Delta\sigma_1 \left[\rho_o(b) - \rho_o(a) \right] - \Delta\sigma_2 \left[\rho_o(b) - \rho_o(a) \right] \right\} \quad .$$

Thus, if $\Delta\sigma_1 = \Delta\sigma_2$ there is no addition, but if $\Delta\sigma_2 << \Delta\sigma_1$ U is nearly twice the voltage generated by one segment.

The condition that $\Delta\sigma_1 >> \Delta\sigma_2$ can be met if the absorption coefficient of region a b is greater than region b c. It is maintained that at the positive and negative peaks this condition is fulfilled for one or the other segment, and the individual photovoltages of alternating segments add to give the observed high photovoltages.

IV. EXPERIMENTAL RESULTS

A. DATA ON SPECTRAL RESPONSE

The data to be presented in the following sections will justify the model set up in the preceding section. The data will be grouped into three categories:

(1) Data which concern the spectral response of the APE

(2) Data which concern the origin of the voltage in individual layers

(3) Other data including results of heat treatment, γ-irradiation, doping and the current-voltage characteristics of the crystals

Regardless of the mechanism which produces the voltage in a single layer of ZnS (strains, for example) this model differs from both Neumark's and Tauc's models in that it assumes that a separate voltage generator exists in each segment. This enables the model to account for the anomalously high voltages at both the positive and negative peaks. In the Neumark and Tauc models, the voltage is generated between the segments, and another mechanism is needed to accomplish the change in polarity (Tauc's doping gradients, Neumark's polarization fields). Thus, an important part of this model is that the two phases can act independently.

1. Spectral Response

The spectral response curve (shown on the following page) is divided into six regions for the following discussion, and for convenience the longer wavelength polarity reversal is denoted by λ_{OR} and the shorter wavelength polarity reversal by λ_{OV}.

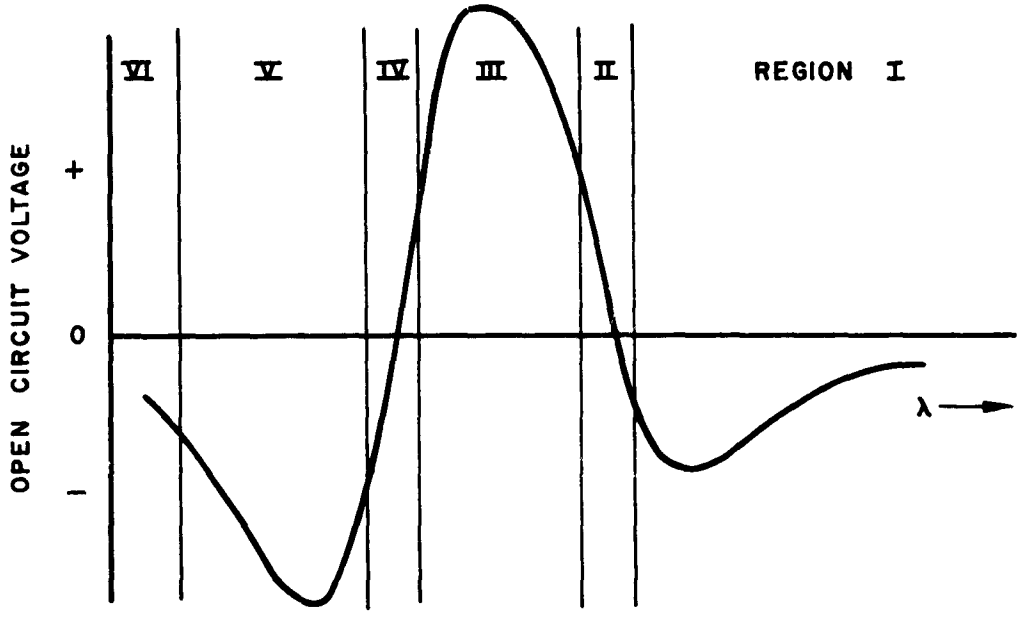

Region	Origin
I	Absorption coefficient of hexagonal region is greater than cubic region.
II	Cubic material absorption increases sharply.
III	"Cubic generators" have maximum output.
IV	Cubic material absorption decreases (in sense of producing carriers); hexagonal absorption is increasing.
V	"Hexagonal generators" have maximum output.
VI	Hexagonal material decreases in absorption.

As mentioned in the text, the transmission curves of hexagonal and cubic material support the proposals for the origins of Regions II and IV, that is, cubic material does begin to absorb in Region II and hexagonal material does begin to absorb in Region IV.

Measurement of the photoconductivity of crystals showing anomalous effects gives evidence to support the proposed origins of Regions IV and VI. The proposed decrease in carrier generation in the cubic phase in Region IV is evidenced by the dip in the photocurrent (Fig. 10a, b) between 335 and 330 mμ. This is just to the short wavelength side of the cubic band gap, and corresponds to Region IV. The decrease in photocurrent below 310 mμ supports the proposed origin of Region VI.

If the origins of Regions I and V are correct, then the photovoltages and currents must be dependent on the polarization of the incident light. It is known[11] that light polarized $\perp$ to the "c" axis is more heavily absorbed than light polarized $\parallel$ to "c" (in hexagonal material). Thus, for the $\perp$ polarization, the voltages and currents should be greater (in absolute value) than for the $\parallel$ polarization. This is precisely what was reported by Cheroff et al.[5] (see Fig. 11a). Moreover, the effect of polarization on the photovoltage and current in Region III can also be predicted from this model. Since the hexagonal "generator" opposes the cubic "generator," then any increase in the hexagonal output in this region will show up as a decrease in the observed voltage in Region III. Then, since cubic material is isotropic, the output in Region III should be <u>greater</u> for light polarized $\parallel$ to "c" than for light polarized $\perp$ to "c." This effect was also observed by Cheroff et al. (Fig. 11a) and was confirmed by Beun and Goldsmith (Fig. 11b). Figures 11a and 11b also show a large shift in λ_{OV} with polarization, while there is no shift in λ_{OR}. According to this model, at λ_{OR} the cubic material is much more absorbing than the hexagonal so that no shift is predicted. On the other hand, at λ_{OV} the hexagonal material is strongly absorbing so that one does expect a shift with polarization.

Fig. 10a Photoconductivity in a Mixed ZnS Crystal

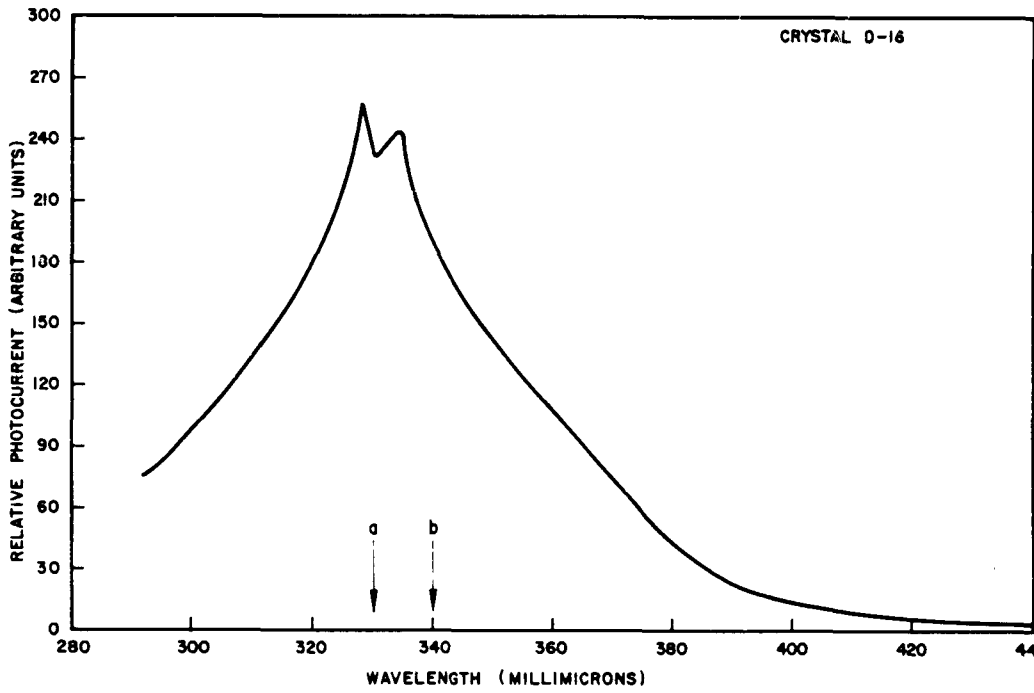

Relative photocurrent of crystal D-16. The dark current at 22.5 vdc is $< 0.001 \times 10^{-10}$ amp. The photocurrent at 330 mμ is $\sim 0.75 \times 10^{-10}$ amp, giving a relative change in conductivity of $\sim$ 750. Arrows "a" and "b" mark positions of hexagonal and cubic absorption edges, respectively.

Fig. 10b Photoconductivity in a Mixed ZnS Crystal

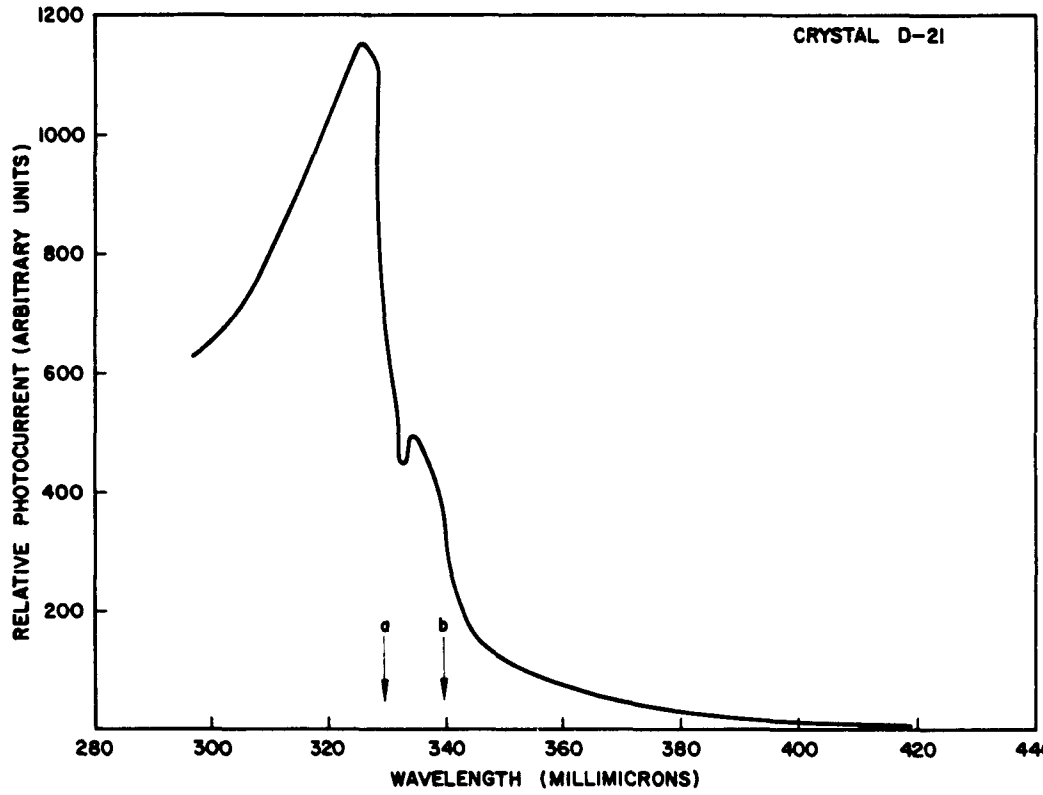

Relative photocurrent of crystal D-21. Arrows "a" and "b" mark positions of hexagonal and cubic absorption edges, respectively.

Fig. 11a Effect of Polarized Light on Photovoltaic Current

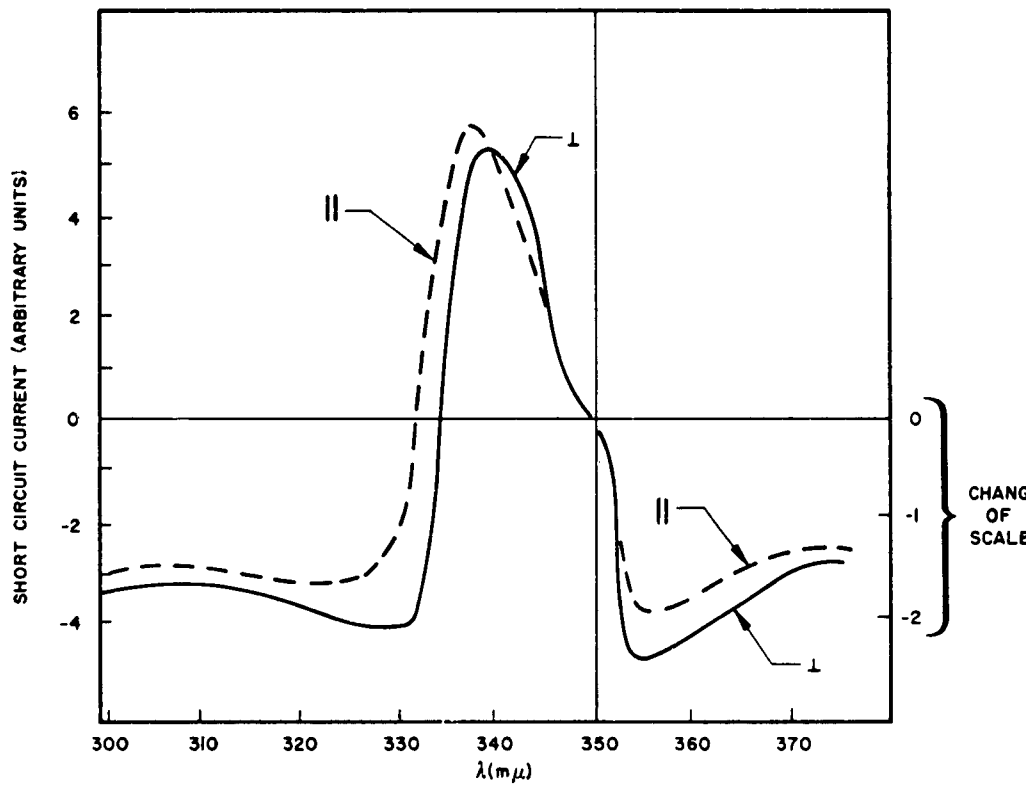

Dependence of spectral response of the photovoltaic current on the polarization of incident light. ⊥ implies the electric vector E of the incident light is perpendicular to "c" axis, ‖ implies E is parallel to "c" [after G. Cheroff, R. C. Enck and S. P. Keller, Phys. Rev. 116. 1091 (1959)].

Fig. 11b Effect of Polarized Light on Photovoltaic Current

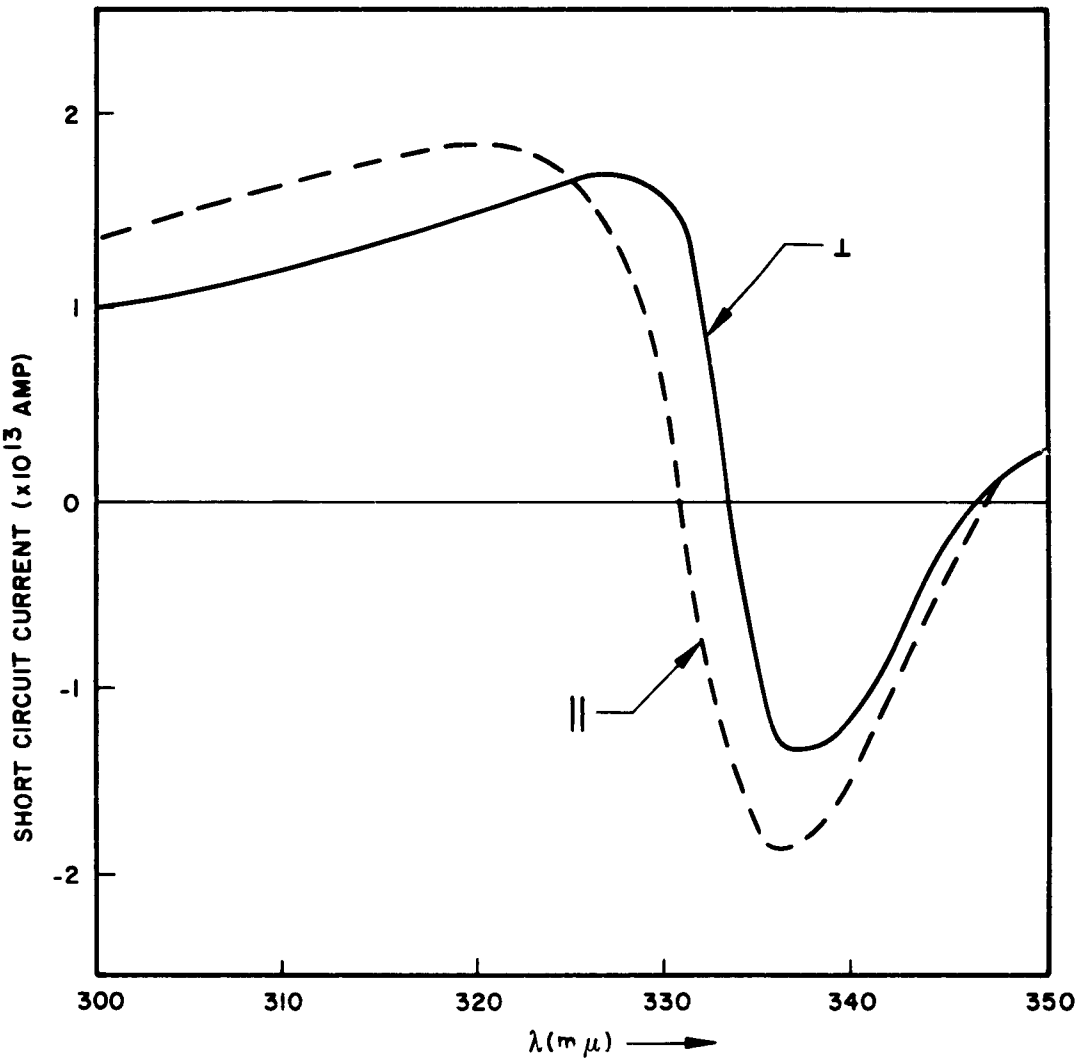

Dependence of spectral response of the photovoltaic current on the polarization of incident light. ⊥ implies the electric vector E of the incident light is perpendicular to "c" axis, ∥ implies E is parallel to "c" [after Beun and Goldsmith, Helv. Phys. Acta 33, 508 (1960)].

2. Polarity Reversals

The positions of the polarity reversals λ_{OR} and λ_{OV} are dependent on the intensity of the incident light (Fig. 12a and b are typical). In fact, in some crystals the polarity reversals disappear altogether at low light levels. The data presented in Fig. 12a, b were taken by adjusting the monochromator and light source for maximum short circuit current at a convenient wavelength and then decreasing the light level by placing copper screens in the light beam. In order to analyze Fig. 12a, b in terms of the proposed model, it is necessary to know quantitatively the variation of the absorption constants with wavelength in this region. However, this same phenomenon can be seen in another experiment. For Fig. 13a, b, the voltages at λ_{OV} and λ_{OR} were measured as the intensity was decreased. Of course, the increase in voltage noted does not continue indefinitely, since the photovoltaic effect must disappear for zero light intensity.

This variation in voltage at λ_{OR} and λ_{OV} can be analyzed in terms of the two-segment unit model. Let the voltage of a two-segment section of the crystal be represented by the following equation:

$$U_n = \ln\left\{\frac{1+\eta_1 I}{1+\eta_1 I u_1}\right\} - \ln\left\{\frac{1+\eta_2 I}{1+\eta_2 I u_2}\right\} , \qquad (20)$$

where U_n is expressed in units of kT/e, I is the maximum light intensity in the experimental set-up, η_1 and η_2 are constants of the cubic and hexagonal segments, respectively. ηI is defined by the relation

$$\eta I = \frac{\Delta\sigma}{\sigma_o} .$$

u_1 and u_2 are related to the fields in the crystal due to the strains and are independent of light intensity. At λ_{OV}, for example,

Fig. 12a Dependence of Red Polarity Reversal on Light Intensity

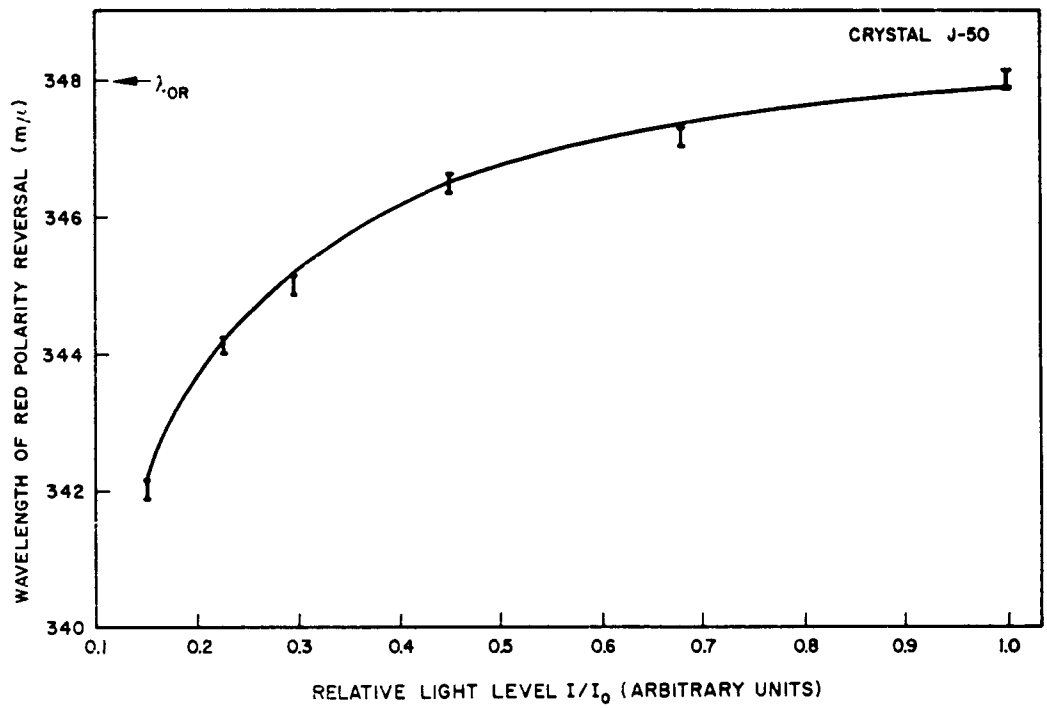

Dependence of the wavelength of red polarity reversal on the intensity of incident light. The maximum light intensity available in the experiment is arbitrarily denoted 1.0.

Fig. 12b Dependence of Violet Polarity Reversal on Light Intensity

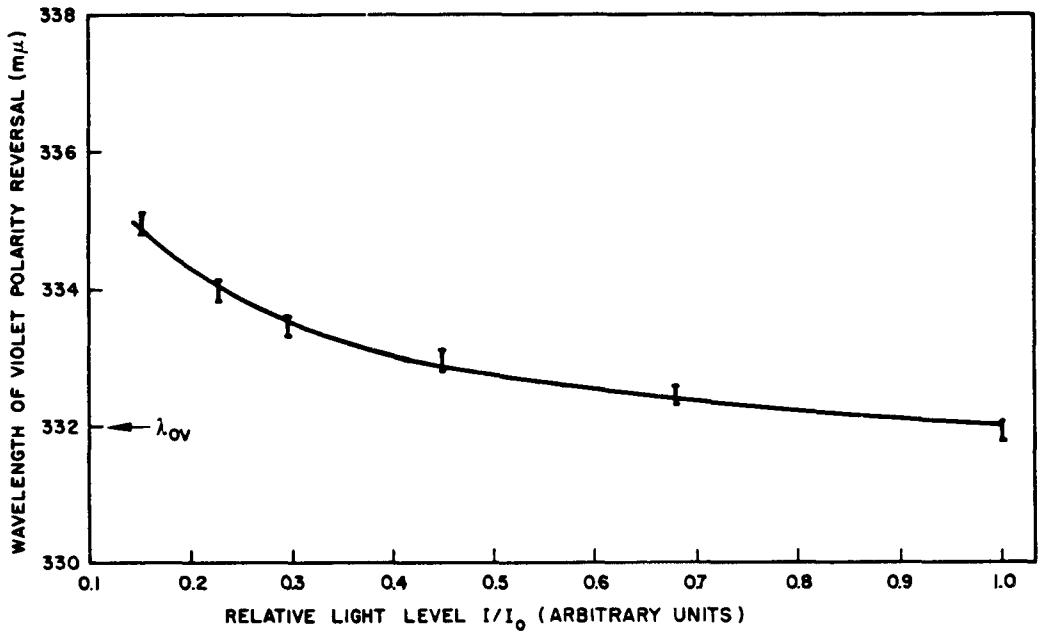

Dependence of the wavelength of violet polarity reversal on the intensity of incident light. The maximum light intensity available in the experiment is arbitrarily denoted 1.0.

Fig. 13a Experimental and Theoretical Dependence of V_{OC} at λ_{OV} on Light Intensity

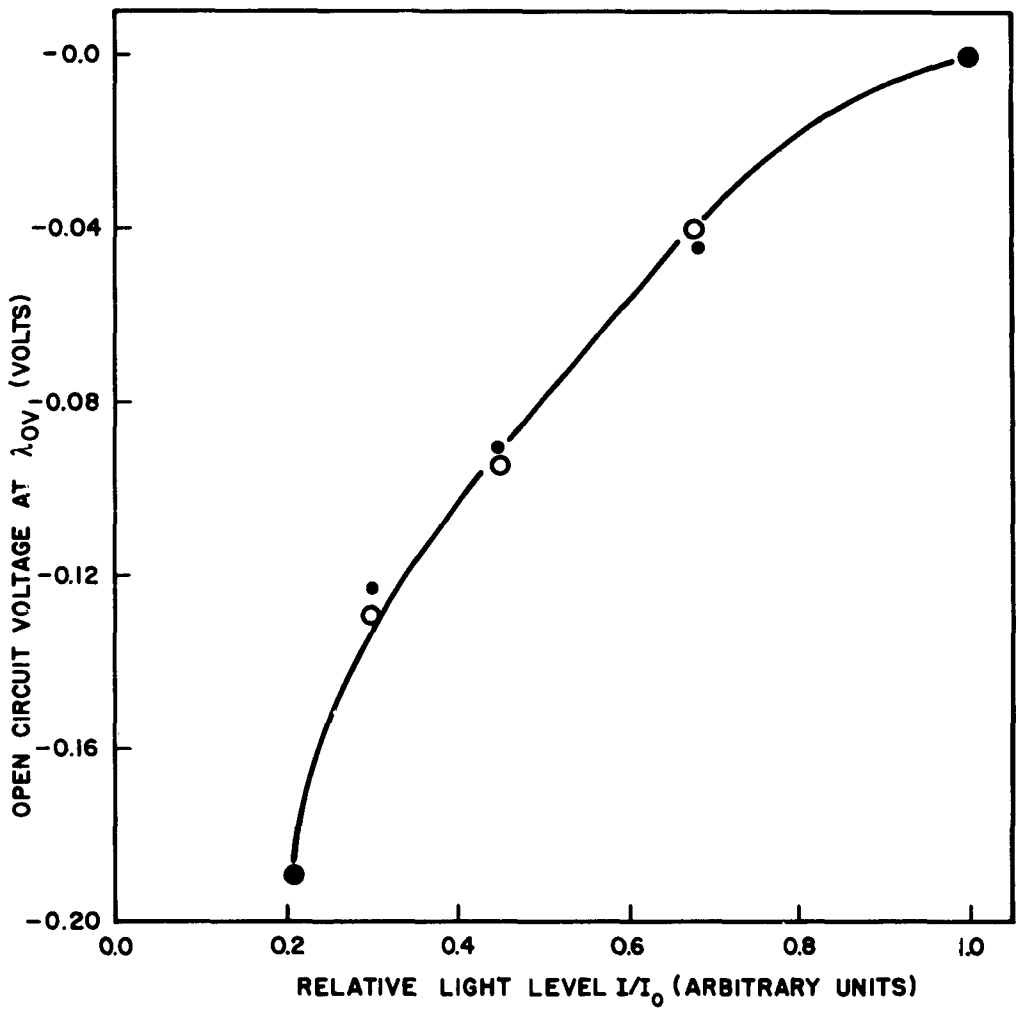

Experimental and theoretical dependence of V_{OC} at λ_{OV} on intensity of incident light. Open circles are experimental points; filled circles are calculated.

Calculated from:

$$V_{OC} = \ln\left(\frac{3.4 - \delta}{3.4 - 0.5\delta}\right); \text{ where } \delta = I_o - I$$

Fig. 13b Experimental and Theoretical Dependence of V_{OC} at λ_{OV} on Light Intensity

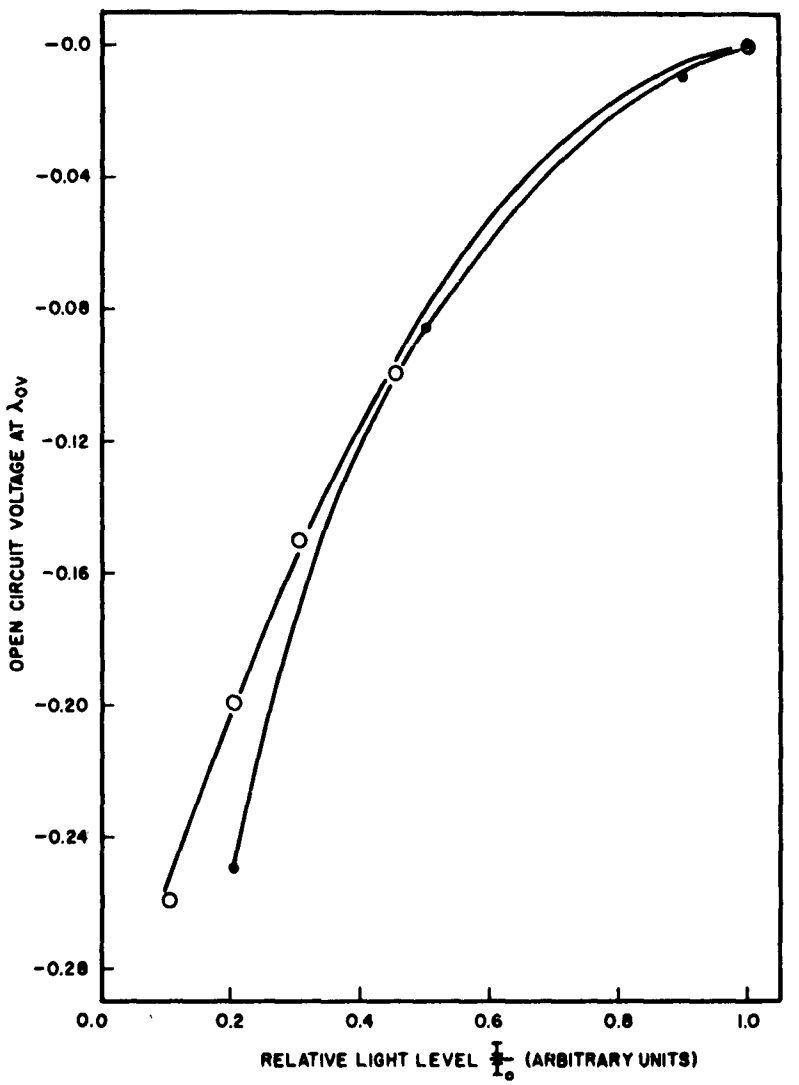

Experimental and theoretical dependence of V_{OC} at λ_{OV} on intensity of incident light. Open circles are experimental points, and filled circles are calculated.

Calculated from:

$$V_{OC} = \ln\left(\frac{1 - 0.9\delta}{1 - 0.8\delta}\right); \text{ where } \delta = I_o - I$$

$$U_n = 0 = \ln \frac{1 + \eta_1 I}{1 + \eta_1 u_1 I} \cdot \frac{1 + \eta_2 I u_2}{1 + \eta_2 I} \quad .$$

Therefore,

$$\frac{1 + \eta_1 I}{1 + \eta_1 I u_1} = \frac{1 + \eta_2 I}{1 + \eta_2 I u_2} \quad . \tag{21}$$

Solving this relation for η_2 ,

$$\eta_2 = \frac{\eta_1 (u_1 - 1)}{\eta_1 I (u_2 - u_1) + u_2 - 1}$$

at λ_o . The following part of the derivation is valid for λ_{ov}. In this region $\Delta\sigma/\sigma_o$ for the cubic phase has decreased so that $\eta_1 I$ is small. Moreover both u_2 and u_1 are of the order of 0.01,* so that $\eta_1 I(u_2 - u_1)$ is negligible compared to $u_2 - 1$. Therefore,

$$\eta_2 \approx \frac{\eta_1 (u_1 - 1)}{u_2 - 1} = \frac{\eta_1 (1 - u_1)}{1 - u_2} > 0 \quad . \tag{22}$$

Now, decrease the light level to I-δ and recalculate U_n at λ_{ov} using Equation (21). Calling this voltage U_n'

$$U_n' = \ln \left\{ \frac{1 + \eta_2 (u_2)(I - \delta) + \eta_1 (I - \delta) + \eta_1 \eta_2 u_2 (I - \delta)^2}{1 + \eta_2 (I - \delta) + \eta_1 u_1 (I - \delta) + \eta_1 \eta_2 u_1 (I - \delta)^2} \right\} \quad . \tag{23}$$

Then, neglecting terms in δ^2 and using relation (21), U_n' becomes

*The voltage generated per layer should be about 0.1 volts[4] or 4 (kT/e) at room temperature. Thus U_n (maximum) = 4 or $\ln u^{-1} = 4$. Thus $u = e^{-4} \cong 0.01$.

$$U_n' = \ln\left\{\frac{1 + \eta_2 I + \eta_1 u_1 I + \eta_1\eta_2 u_1 I^2 - \delta\left(\eta_1 + \eta_2 u_2 - 2\eta_1\eta_2 u_2 I\right)}{1 + \eta_2 I + \eta_1 u_1 I + \eta_1\eta_2 u_1 I^2 - \delta\left(\eta_2 + \eta_1 u_1 - 2\eta_1\eta_2 u_1 I\right)}\right\} .$$

The equation has the form

$$U_n' = \ln\left\{\frac{a - b\delta}{a - c\delta}\right\} , \tag{24}$$

where

$$\left.\begin{aligned} b &= \eta_1 + \eta_2 u_2 - 2\eta_1\eta_2 u_2 I \\ c &= \eta_2 + \eta_1 u_1 - 2\eta_1\eta_2 u_1 I \end{aligned}\right\} . \tag{25}$$

Then, using Equation (22) and Equations (25),

$$\frac{b}{c} = \frac{\eta_1\left(1 - u_2\right) + \left(1 - u_1\right)\left(\eta_1 - 2\eta_1^2 u_2 I\right)}{\eta_1 u_1\left(1 - u_2\right) + \left(1 - u_1\right)\left(\eta_1 - 2\eta_1^2 u_1 I\right)} , \tag{26}$$

but, following the reasoning leading to Equation (22), Equation (26) can be re-written as

$$\frac{b}{c} = \frac{\eta_1\left(1 - u_2\right) + \eta_1\left(1 - u_1\right)}{\eta_1 u_1\left(1 - u_2\right) + \eta_1\left(1 - u_1\right)} = \frac{2 - u_1 - u_2}{1 - u_1 u_2} . \tag{27}$$

This equation is symmetric in u_1 and u_2 and since both u_1 and u_2 are < 1, it is easily seen that $\frac{b}{c} > 1$.

Thus,

$$0 < \frac{a - b\delta}{a - c\delta} < 1$$

for small δ , and

$$U_n' = \ln\left(\frac{a - b\delta}{a - c\delta}\right) < 0 ,$$

i.e., the voltage goes negative as δ increases.

The best fitting expressions of the form of Equation (24) are shown on Fig. 13a, b. These are just empirical fits and little significance can be tied to the various values of a, b and c used in these equations. It must be remembered that in this derivation, only the voltage due to two segments of the crystal was calculated. Actually, the crystal is made of many such layers, all slightly different. Thus, the experimental data is just the resultant of the actions of many slightly different sets of segments.

3. Dependence of λ_{OV} on the Elemental Photovoltage

According to the proposed model, one would expect that the relative magnitudes of the positive and negative peaks would have an effect on the position of λ_{OV}. Qualitatively, if the positive peak is much larger than the negative peak, then the positive peak voltage should persist to shorter wavelengths. Such a crystal would have λ_{OV} much farther in the violet than a crystal in which the positive and negative peaks are of comparable magnitude. The wavelength λ_{OV} versus the ratio of the magnitudes of the positive and negative peak voltages is shown in Fig. 14 for a number of crystals. The scatter of the data is large, but one observes a definite trend of the type outlined above.

This trend has a quantitative basis. To show this relation, assume that at the positive and negative peaks the observed voltage is saturated. Then, the observed

positive and negative peak voltages V_+ and V_-, respectively, are

$$V_+ = n \frac{kT}{e} \ln \frac{1}{u_1} ,$$

$$V_- = -n \frac{kT}{e} \ln \frac{1}{u_2} ,$$

where n is just half the number of segments in the crystal, and u_1 and u_2 are functions depending only on the strain and piezoelectric constants. Also, let r be defined as the ratio of the magnitudes of V_+ and V_-

$$r = \frac{V_+}{|V_-|} = \frac{\ln 1/u_1}{\ln 1/u_2} ,$$

then

$$r \ln \frac{1}{u_2} = \ln \frac{1}{u_1} ,$$

and

$$u_1 = u_2^r . \tag{28}$$

But, since we are interested only in λ_{OV}, use condition (22) from the preceding section.

Then,

$$\eta_2 = \eta_1 \frac{\left(1 - u_2^r\right)}{1 - u_2} \tag{29}$$

since $\eta_2 = \frac{\Delta\sigma_2}{I\,\sigma_{2o}}$, η_2 is proportional to the absorption coefficient of hexagonal ZnS and varies inversely with wavelength. In fact Beun and Goldsmith[11] find that the absorption coefficient α varies with $(h\nu)^2$. Thus,

$$\eta_2 \approx \frac{1}{\lambda^2}$$

and Equation (29) becomes

$$\lambda^2 \approx \frac{1}{\eta_1}\left(\frac{1 - u_2}{1 - u_2^r}\right)$$

or,

$$\lambda \approx \sqrt{\frac{1}{\eta_1}}\sqrt{\frac{1 - u_2}{1 - u_2^r}} \quad , \tag{30}$$

r being always greater than zero. Since $r = 0$ implies $V_+ = 0$, this means that there is no sign reversal and λ_{OV} is not defined. Figure 15 is a plot of Equation (30) for various values of u_2 and should be similar in form to the data presented in Fig. 14. In Fig. 14, u_2 is not constant. Figure 15 shows that the largest spread between curves with different u_2 occurs for small values of r. This is apparently the case in Fig. 14. Also the trend predicted by Equation (30) shows up in Fig. 15. Admittedly, the agreement is not excellent, but it must be remembered that the calculation was done for an ideal model consisting of n identical segments of hexagonal and n identical segments of cubic material. Visual observation of ZnS crystals reveals that in a real crystal the sizes of the layers are rather random. Thus, the scatter in points on Fig. 14 is hardly unexpected.

Fig. 14 Relation Between λ_{OV} and r

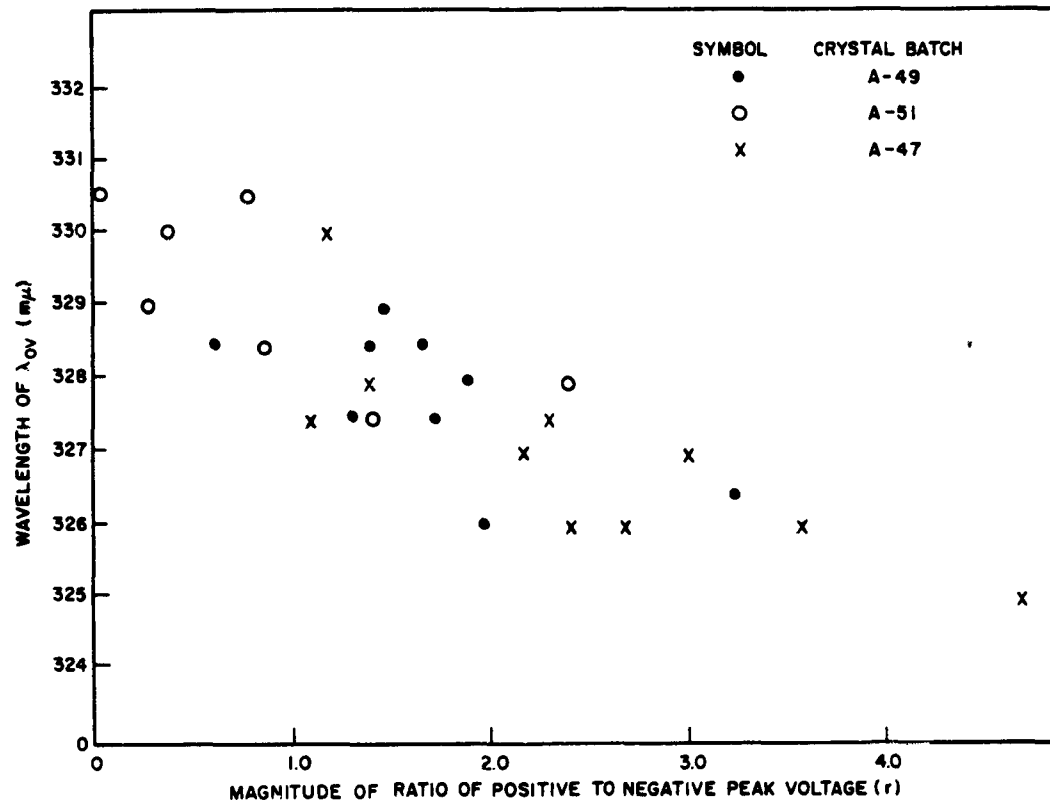

The wavelength of the violet polarity reversal vs. the absolute magnitude of the ratio of the maximum open-circuit voltage at the positive peak to the maximum value of the open-circuit voltage at the negative peak. This ratio is denoted r.

Fig. 15 Calculated Relation Between λ_{OV} and r

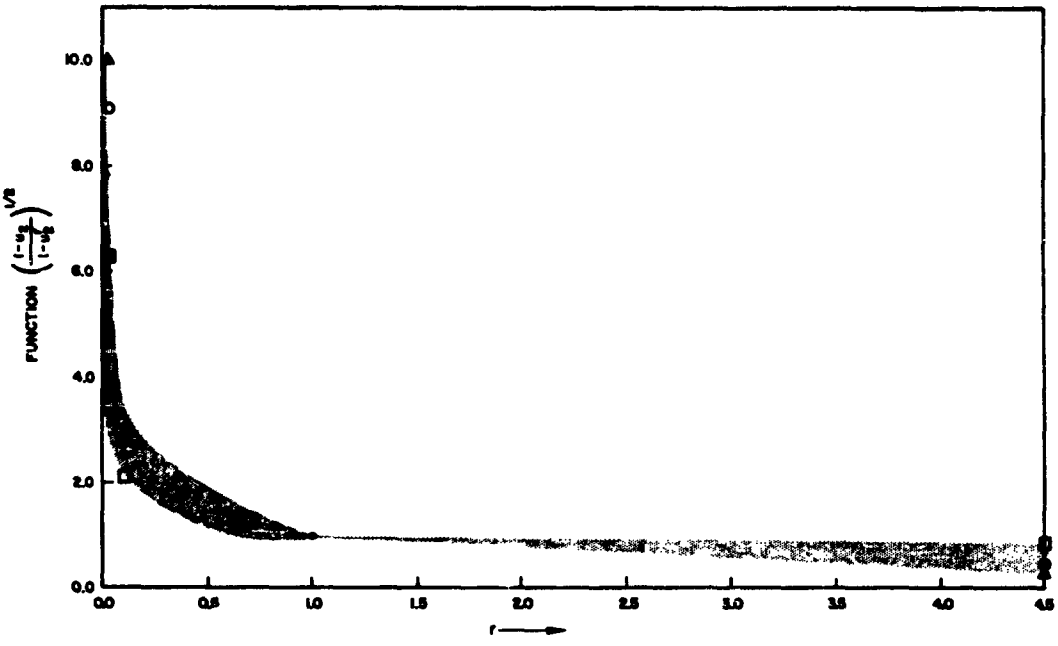

Furthermore, Equation (30) was calculated assuming that the positive and negative peak voltages are saturated. Experimentally, it was not always possible to saturate the photovoltages.

4. Temperature Dependence of the Spectral Response

Cheroff[28] has measured the temperature dependence of the spectral response. Two pieces of data are forthcoming. First, that the voltage increases at low temperatures according to the relation

$$V_{OC} \sim \ln \frac{1}{T} \cdot$$

Second, the difference in energy ΔE between λ_{OV} and λ_{OR} increases linearly with temperature. The slope at low temperature is $\Delta E/kT = 3.7$, and above room temperature the slope is $2\Delta E/kT$. According to the proposed model, λ_{OR} is associated with the cubic band gap and λ_{OV} is associated with the hexagonal band gap. Thus, the change with temperature of

$$-\Delta E = \frac{hc}{\lambda_{OR}} - \frac{hc}{\lambda_{OV}}$$

is just given by the difference in dEg/dT between the cubic and hexagonal phases and should correspond to the slope of the ΔE vs. T curve of Cheroff. Above room temperature this difference is just $\Delta E = 2kT$ (Ref. 29).

B. EVIDENCE OF ORIGIN OF PHOTOVOLTAGE

Thus far the evidence presented has only established the fact that the spectral response of the photovoltage can be accounted for on the basis of the proposed model. However, nothing has been said of the origin of the voltage in each

segment. The following sections will present evidence that the elemental photovoltages are due to piezoelectric fields induced by permanent non-uniform internal strains.

1. Measurements on Mixed Crystals

There is some very qualitative evidence that the voltage generators are associated with some property of the crystal structure. It is found that in the majority of crystals studied, the end of the crystal grown last is positive when illuminated with light of wavelength ~340 mμ . This result is supported by Merz.[4] Moreover, it was also found that when a compressional strain is applied in the dark along the long axis of the crystal, a piezoelectric voltage is generated. The end of the crystal which becomes positive under compression is identical with the end of the crystal which is positive at 340 mμ. Lempicki[17] found a one-to-one correspondence between the polarity of the positive peak and the pyroelectric voltage.

In order to test the postulate that strain-induced piezoelectric fields are the voltage-producing mechanisms in the crystal, the spectral response of the APE was measured on crystals with a longitudinally applied stress. The stress was always compressional, since the crystals are too weak to stress in tension.

To analyze the effect of application of an applied stress on the crystal, consider the figure on the following page. The solid line represents the variation of the transverse lattice constant on passing from one phase to the other. Suppose a uniform stress Π is applied to the crystal. Then in the bulk of each segment, the lattice dilates. The dilation in Region I is δ_1 and in Region II is δ_2 (again, assume a linear gradation in lattice constant from the hexagonal to cubic phase).

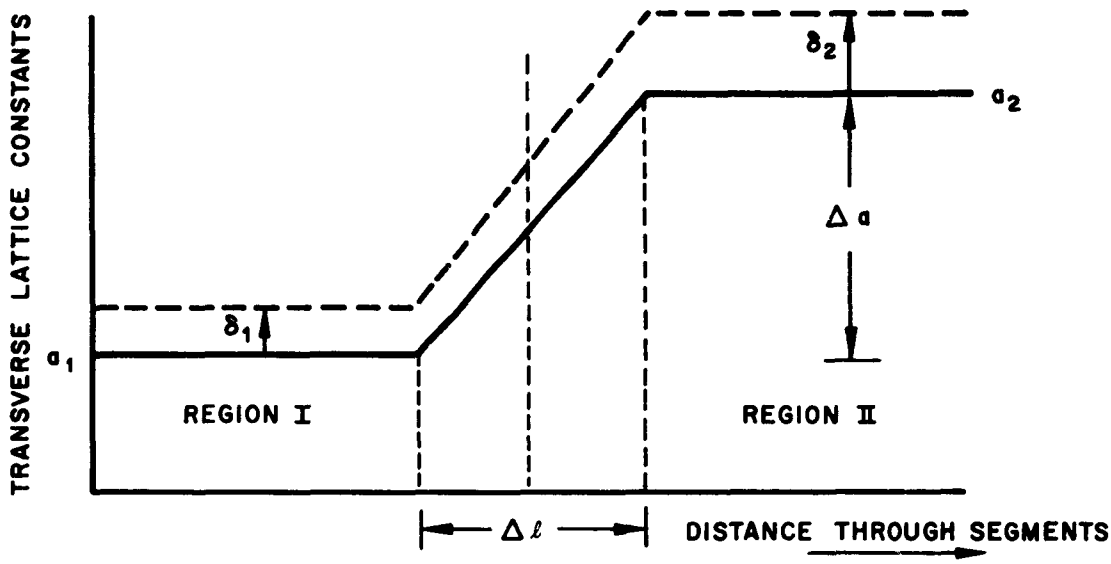

Then, if this slope before application is

$$\Delta a/\Delta \ell$$

then, after an applied stress it is

$$\frac{\Delta a'}{\Delta \ell} = \frac{\Delta a + \delta_2 - \delta_1}{\Delta \ell} .$$

But, since the stress is uniform,

$$\delta_1 c_1 = \delta_2 c_2 \quad \text{and} \quad \delta_2 = \delta_1 c_1/c_2 ,$$

where c_1 and c_2 are the appropriate elastic constants. Thus.

$$\frac{\Delta a'}{\Delta} = \frac{\Delta a + \delta_1 \left(\frac{c_1}{c_2} - 1 \right)}{\Delta \ell} .$$

The stress Π is

$$\Pi = \delta_1 c_1 ,$$

and

$$\delta_1 = \Pi / c_1 ,$$

therefore.

$$\frac{\Delta a}{\Delta \ell} = \frac{\Delta a + \Pi \left(\frac{1}{c_1} - \frac{1}{c_2} \right)}{\Delta \ell} .$$

Unfortunately, values for both c_1 and c_2 are not available. Thus, it cannot be predicted whether the slope increases or decreases.

With that difficulty in mind, some analysis of the effect of strain can be made. As in the section on intensity, consider a two-segment section of the crystal and represent the resultant voltage as

$$U_n = \ln \frac{1 + a_1}{1 + a_1 e^{-\alpha_1}} \cdot \frac{1 + a_2 e^{-\alpha_2}}{1 + a_2} ,$$

where U_n is in units of kT/e, a_1 and a_2 are $\Delta\sigma/\sigma_o$ for each phase, and $e^{-\alpha_1}$ and $e^{-\alpha_2}$ are the functions depending on strain gradient, etc. Then apply a small stress p. U_n becomes

$$U_n' = \ln \left(\frac{1 + a_1}{1 + a_2} \right) \frac{1 + a_2 e^{-\alpha_2 + \nu_1 p}}{1 + a_1 e^{-\alpha_1 + \nu_2 p}} ,$$

where ν_1 and ν_2 are constants.

At λ_{OV}, $U_n = 0$ so that

$$\frac{1 + a_1}{1 + a_2} \cdot \left(\frac{1 + a_2 e^{-\alpha_2}}{1 + a_1 e^{-\alpha_1}} \right) = 1 \ .$$

Then, if the applied stress is small,

$$e^{\nu_1 p} \approx 1 + \nu_1 p \ ,$$

and U_n' can be rewritten

$$U_n' = \ln \left\{ \frac{(1 + a_2)(1 + a_1 e^{-\alpha_1}) + a_2 e^{-\alpha_2} \nu_2 p}{(1 + a_2)(1 + a_1 e^{-\alpha_1}) + a_1 e^{-\alpha_1} \nu_1 p} \right\} \ . \qquad (31)$$

This equation has the form

$$\ln \left(\frac{A + bp}{A + cp} \right) \ . \qquad (32)$$

The argument of Expression (32) has the form

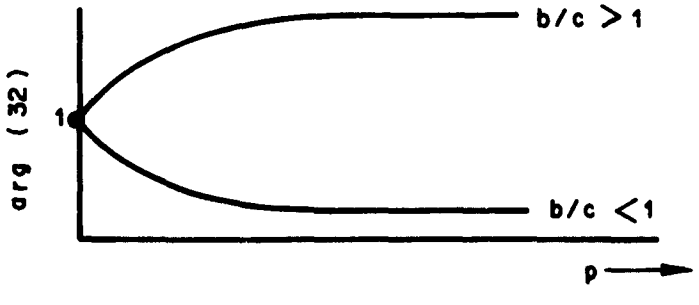

Thus, for either case U_n' will saturate. This is just what was found. The best data taken at λ_{OV} is shown in Figs. 16 and 17. As with the light intensity data, the results are presented in two ways: (1) as a shift in λ_{OV}, Fig. 16, and (2) as a change in voltage at λ_{OV}, Fig. 17.

2. Experiments on Single Crystal ZnS

Since the results of the last section show an uncertainty in the predicted polarity of the voltage generated at λ_{OV} by an applied uniaxial stress, an experiment was devised using single crystal ZnS to test directly the origin of the photovoltage in one layer of a mixed crystal. The experiment was preformed on a single crystal of hexagonal ZnS. A similar experiment was attempted on cubic material, but it was found that the resistivity of the material available was so low that the crystal showed no piezoelectric properties.

The experiment consisted of non-uniformly stressing the crystal and then observing the photovoltage generated when the strained crystal was illuminated with ultraviolet light. The contribution to the photovoltage due to contacts was taken into account by noting the photovoltage in the unstrained crystal and subtracting off this effect.

In order to interpret the results of this experiment, one needs a model of the strain pattern in the mixed crystal. This subject was touched on in Section III-B, where it was pointed out that the hexagonal-to-cubic transition is much less abrupt than the cubic-to-hexagonal transition, and that the strain gradients will be smaller at the hexagonal-to-cubic transition. It will be assumed, in keeping with the qualitative nature of this work, that these photovoltages are negligible in comparison to the photovoltages generated at the cubic-to-hexagonal transition. Thus, in a mixed crystal, the photovoltages associated with the

Fig. 16 Shift of λ_{OV} With Applied Stress

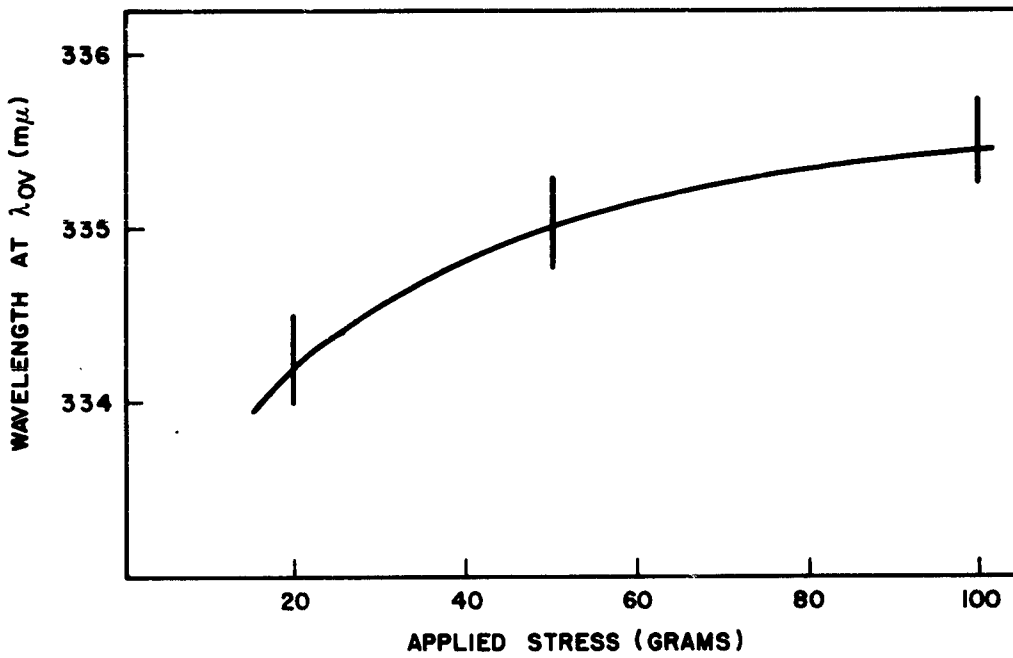

The shift in position of the violet polarity reversal with compressional stress applied along the "c" direction.

Fig. 17 Open-Circuit Voltage at λ_{OV} as a Function of Applied Stress

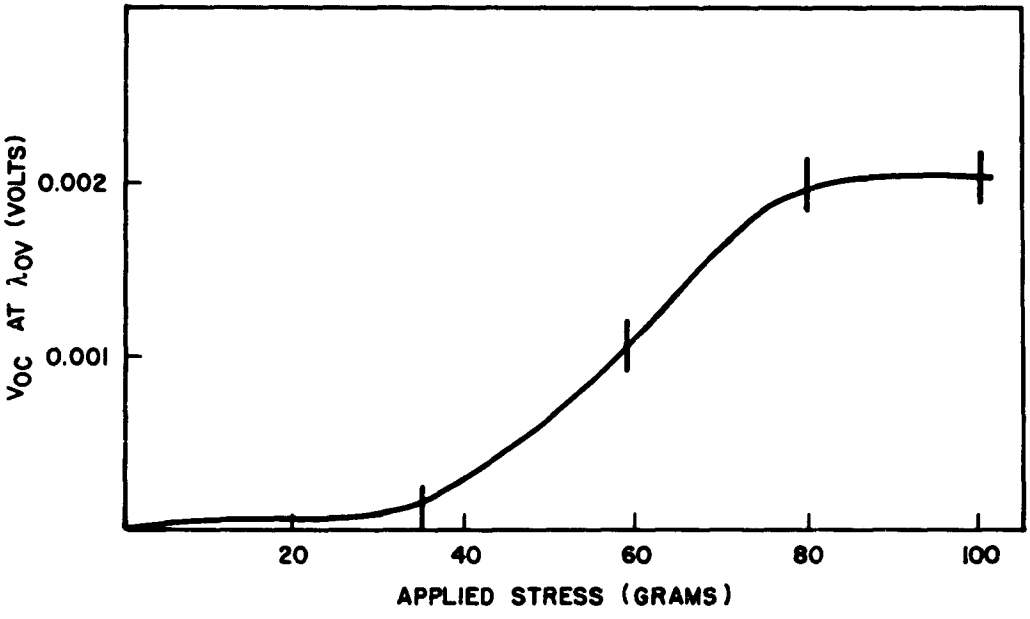

The change in voltage at the violet polarity reversal with compressional stress applied along the "c" direction.

hexagonal layers will be due to a strain gradient which, in each hexagonal layer, decreases in the direction of crystal growth.

It was pointed out in Section I-C that Merz[4] found a relation between the direction of crystal growth and the polarity of the photovoltage at 340 mμ. This result was confirmed for the vast majority of crystals examined in this study and it was found that the end of the crystal grown last was always positive when illuminated with light of wavelength corresponding to the positive peak. Lempicki's result[17] that the end of the crystal which became positive on heating (secondary pyroelectric effect) was also positive when illuminated with light of wavelength 340 mμ (the positive peak) is also necessary to the interpretation of this experiment. Since only the hexagonal phase is pyroelectric,[30] this effect allows one to orient the hexagonal single crystal, relative to its orientation in the mixed crystal.

To summarize: it is now evident that the hexagonal layers in the mixed crystals are so oriented that the strain gradients in these layers decrease toward that end of the crystal which becomes positive when illuminated with light corresponding to the positive peak. Furthermore, the "c" axis is so oriented that on heating (secondary pyroelectric effect) the end of the crystal which becomes positive is identical with the end which becomes positive when the crystal is illuminated with light corresponding to the positive peak. Thus, in the single crystal, the strain should decrease in the direction of the secondary pyroelectric effect on heating.

In carrying out the experiment, the direction of the secondary pyroelectric effect was found by using the dynamic method described by Chynoweth.[31] When this direction was identified, the crystal was ground to the shape shown on the following page.

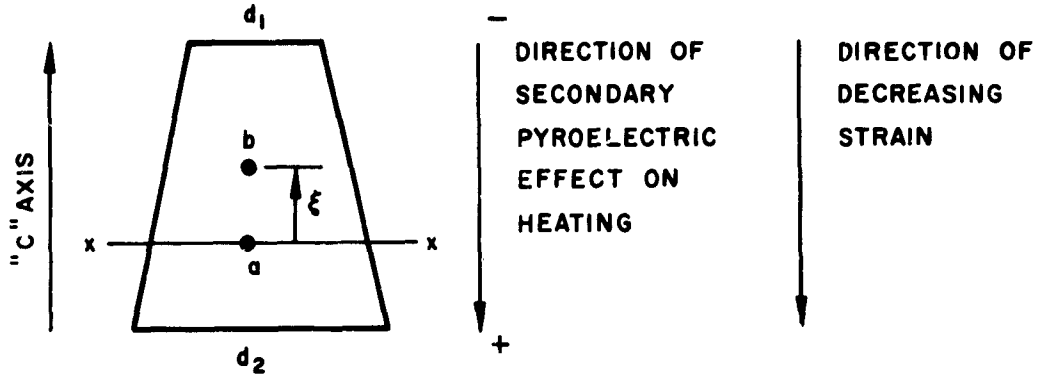

A stress was then applied perpendicular to the "c" axis and perpendicular to the trapezoidal face of the crystal. In this manner, a strain gradient of the transverse lattice constants can exist along the "c" axis when the center-of-mass of the load is not directly above the centroid of the trapezoidal face of the sample. For this case, the stress gradient $d\sigma/dx$ is given by the relation[32]

$$\frac{d\sigma}{dx} = \frac{F\xi}{I_{xx}} ,$$

where F is the applied force, ξ the distance on the face of trapezoid between the center-of-mass of the load (b) and the centroid of the sample (a). I_{xx} is the moment of inertia about the line x-x. The photovoltage was measured between faces d_1 and d_2. This configuration was used instead of one in which the stress was applied along "c," so that the observed photovoltage would involve only the transverse piezoelectric constants and not the longitudinal piezoelectric constants.

When the stress was applied and the sample illuminated, a net photovoltage of approximately 4 mv was observed. The polarity was such that contact d_1 was positive with respect to d_2. That is, the polarity is opposite the polarity associated with the secondary pyroelectric effect on heating, and therefore, the

polarity associated with the positive peak photovoltage. This is precisely the required result, since, in the model, the photovoltage due to the hexagonal layers in the mixed crystal is associated with the negative peak.

The value of the photovoltage one expects in this experiment can be calculated using the expression derived for U in Section III-B.2.c. From this equation the maximum value of the photovoltage is found to be

$$U_m = gsa^2 \, d\Pi/dx \, .$$

The piezoelectric constant g was measured on the same sample used in this experiment and was found to be 2.7×10^{-9} (v-cm/dyne).* Using this value for g the maximum value of the photovoltage expected for the configuration used in the experiment is

$$U_m = 3.4 \times 10^{-3} \text{ volts} \, .$$

This value appears to be slightly too low but it must be remembered that a strain gradient can also produce a photovoltage by virtue of the band gap change produced by the strain gradient. This effect was investigated by Tauc.[22] On the basis of his calculation and using a value of dEg/dP from Ref. 29, this contribution to the photovoltage is -0.6×10^{-3} volts. Note this voltage is of the opposite polarity from the voltage observed. Thus, including this correction in the calculation of the photovoltage in a strained crystal, one finds that the observed photovoltage should be 4×10^{-3} volts. This is just the voltage which was observed.

*For the sake of completeness, the longitudinal piezoelectric constant g_{33} was measured and found to be 5.1×10^{-9} (v-cm/dyne).

The agreement between the two voltages is probably better than is warranted, due to errors involved in the experiment. For instance, the quantity ξ in the stress gradient expression was very difficult to measure and could be in error by 50%. Thus, the agreement is probably no better than order-of-magnitude agreement. However, the experiment still shows that the observed polarity of the photovoltage is of the right polarity to account for the voltage at the negative peak and that the calculations in Section III-B. 3 give better than order-of-magnitude agreement with the experiment.

V. OTHER RESULTS

This section will be devoted to the presentation and discussion of experiments which yield results that were not reproducible. That is, either the experiment was not repeatable on the same crystal and/or with different crystals (with similar photovoltaic properties). Since the magnitude of the effects observed varied greatly between crystals, it was felt necessary that measurements should always be repeated for a number of crystals. By and large, the data presented in this section are the results of experiments in which no consistence could be found between crystals. The experiments which fell into this category were as follows:

1) The Study of Surface Conditions
2) The Effect of γ-radiation on the APE
3) Effects of Diffusion of Ag into Crystals and Heat Treatment
4) Effects of Addition of Cu to Starting ZnS
5) Current Voltage Characteristics of Crystals Showing APE

A. THE STUDY OF SURFACE CONDITIONS

In an attempt to study the role played by surface conditions on the APE, a number of crystals whose spectral response characteristics were known were subjected to a mild sandblasting perpendicular to the "c" axis, using micron-sized aluminum oxide powder. After the first treatment, most of the crystals showed a decrease in the short-circuit current. The open-circuit voltage either remained constant or increased. The overall shape of the spectral response curve appeared to be unchanged. The decrease in the short-circuit current is attributable to a loss in the number of hole-electron pairs created by the incident light. The decrease in the number of hole-electron pairs may be attributed to either one or both of the following causes. First, the reflection losses

at the surface will be increased by the irregularities produced on the surface by the grit. Second, since the surface-to-volume ratio of a typical crystal is about 50 cm^{-1}, surface recombination might be expected to be important in determining the lifetime of excess carriers. Generally, sandblasting a surface increases the surface recombination and thus, decreases the lifetime of the excess carriers. Since in the steady state the number of excess carriers N is related to the lifetime τ and the generation rate f by[33]

$$N = f\tau,$$

a decrease in the excess carrier concentration will result from a decrease in τ. This leads to a decrease in the short-circuit current

The increase in the open-circuit voltage could be due to an increase in the amount of disorder in the crystal (i.e., the number of segments). It has been found that even mild pressure, applied at a point perpendicular to the "c" axis, induces additional disorder in the vicinity of the stress.* In fact, a number of crystals developed cracks transverse to the "c" axis as a result of the sandblasting. There was no consistency in the results of further sandblasting, except that most crystals developed transverse cracks.

B. THE EFFECT OF γ - RADIATION ON THE APE

A number of crystals were irradiated with Co^{60} gamma rays. Two irradiations were made, one at a flux density of 5×10^5 r/hour and the other at 5×10^4 r/hour. The integrated doses were 10^8 r and 10^5 r, respectively. The purpose of these irradiations was to try to study the effect of impurities on the APE.

*J. Singer, Private Communication, General Telephone Co.

Co^{60} gamma rays will produce vacancy-interstitial defects which can act as donors or acceptors. After irradiation to 10^8 r, the crystals displayed no anomalous photovoltaic effects. That is, high photovoltages and polarity changes were absent. In addition, it was noted that the conductivity of these crystals increased by factors of the order of 10^5. This increase in conductivity could well be the cause of the disappearance of the APE. As the model is presented here, this connection is not evident. This follows from the approximations made in the derivation of the photovoltage for a single segment of the crystal. It was necessary to make these approximations in order to obtain a solution in closed form. However, it is well known that a crystal of low resistivity will show no piezoelectric properties.[34] Thus, the disappearance of the APE in these crystals may well be due to the shorting out of the piezoelectric properties of these crystals by the increased conductivity.

A calculation of the Debye length[35] for irradiated and unirradiated crystals gives some substance to this argument. For a typical crystal ($\rho \sim 10^{10}$ Ω-cm), the Debye length is approximately 0.2 cm. However, in an irradiated crystal, the Debye length is decreased by a factor of about $\left(\sqrt{10^5}\right)^{-1}$ to a value of approximately 7×10^{-4} cm. Merz[4] estimates that the segments in an anomalous crystal are of the order of 10^{-3} cm long. Thus, the Debye length in an irradiated crystal is of the order of, or less than, the length of a representative segment of the crystal. This makes the presence of a piezoelectric field in such a segment somewhat unlikely.

Among the crystals which were irradiated to 10^5 r, the effects were not as drastic. In all cases, the short-circuit current increased in the vicinity of the negative peak. In both the positive peak region and the long wavelength region

($\lambda > \lambda_{OR}$), the behavior was varied. There appeared to be no correlation between changes in current in one region with changes in another.

The open-circuit voltage also changed with irradiation. It was found that if the voltage at wavelengths corresponding to the negative peak increased, the voltage at the positive peak decreased. The converse was also true. This conforms to the model, in that it is postulated that the generators in adjacent layers are opposed. Thus, for the purposes of discussion, suppose that the generators in the hexagonal regions increase their output. Then in the region of the positive peak (i.e., the region associated with the cubic segments), the photovoltage should decrease, since any contribution from the hexagonal layers is of the opposite polarity. Furthermore, the absolute magnitude of the change in voltage at the positive peak is always close to one-half the change in voltage at the negative peak.

The changes in the positions of the polarity reversals were not consistent.

C. EFFECTS OF DIFFUSION OF Ag INTO CRYSTALS AND HEAT TREATMENT

In another attempt to study the effects of impurities on the APE, silver (in the form of silver sulfide) was diffused into crystals with known spectral responses.[36] The diffusion was carried out at about 600°C. The results were entirely erratic, most of the crystals losing their anomalous properties. The conditions of the experiment were not well controlled, as it was necessary to remove the electrical contacts from the samples before the diffusion. Since the crystals are small, it was not possible to replace the contacts in exactly the same place. This, in itself, can change the spectral response of the crystals (since different segments may be shorted out by the electrode material). Furthermore,

it is known that heat treatment can change the structure of ZnS (Ref. 37). Thus, it was not possible to separate the effects of heat treatment from the effects of doping

D. EFFECTS OF ADDITION OF Cu TO STARTING ZnS

A number of crystals were grown from ZnS to which Cu had been added.[5] Several batches of crystals were grown with doping concentrations ranging from 10^{-3} to 5×10^{-5} gm Cu per gm of ZnS. Data was taken on approximately ten crystals from each batch. In general, the spectral response curves of crystals from different batches were very similar. No correlation was found between the impurity concentration in the starting ZnS, any significant experimental quantity (such as λ_{OV}, λ_{OR}), and the position and magnitude of the positive and negative peaks. It cannot be stated unequivocally that the concentration of impurities in the crystals was even proportional to the concentration of impurities in the starting material. On this basis it is felt that no conclusions can be drawn from this data.

E. CURRENT-VOLTAGE CHARACTERISTICS OF CRYSTALS SHOWING APE

The current-voltage characteristics of crystals having similar photovoltaic properties fell into two classes. None of the current-voltage characteristics depended on the material used to make electrical contact to the crystals. The applied voltages ranged from millivolts to 280 volts. For very low voltages (< 10 volts) most crystals displayed ohmic characteristics. At higher voltages the behavior is varied. The two categories of behavior are as follows:

1) Ohmic to V^n dependence
2) Current saturation at high voltage

1. Square Law Behavior

Only two samples displayed current-voltage (I - V) characteristics expressible by an equation of the form

$$I = (\text{constant})\ V^n .$$

The spectral response of the APE in these crystals was of the type shown in Fig. 1. One sample (L-10) remained ohmic to 40 volts (approximately 200 v/cm). Above 40 volts the current varied as V^2. The other sample (J-5) remained ohmic to about the same voltage and then changed to a behavior expressible as $I = (\text{const.})\ V^{1.2}$. The current-voltage characteristics of sample (L-10) is that of a trap-free solid whose high field conductivity is limited by space charge effects. The agreement between the theory for space charge limited currents and the data presented in Fig. 18 is evident from the following numerical calculations. Lampert[38] relates the break point voltage (that is, the voltage at which space charge effects begins to take over the conduction mechanism) $V(\Omega - s)$, the resistivity ρ, the dielectric constant ϵ, the mobility μ and the electrode spacing ℓ in the following equation:

$$V(\Omega - s) = \frac{10^{13}\ell^2}{2\epsilon\mu\rho} \text{ (volts)} .$$

With $\epsilon = 10$, $\mu = 1$, $\ell = 0.2$ cm, $\rho = 4.4 \times 10^8$ Ω-cm (as determined from the initial slope of the curve), this equation yields a value of $V(\Omega - s)$ of 50 volts. The experimental value is 44 volts. Furthermore, a calculation of the current at a high voltage, according to an equation given by Bube[39] gives, for the total current J,

Fig. 18 Current-Voltage Plot for Crystal L-10

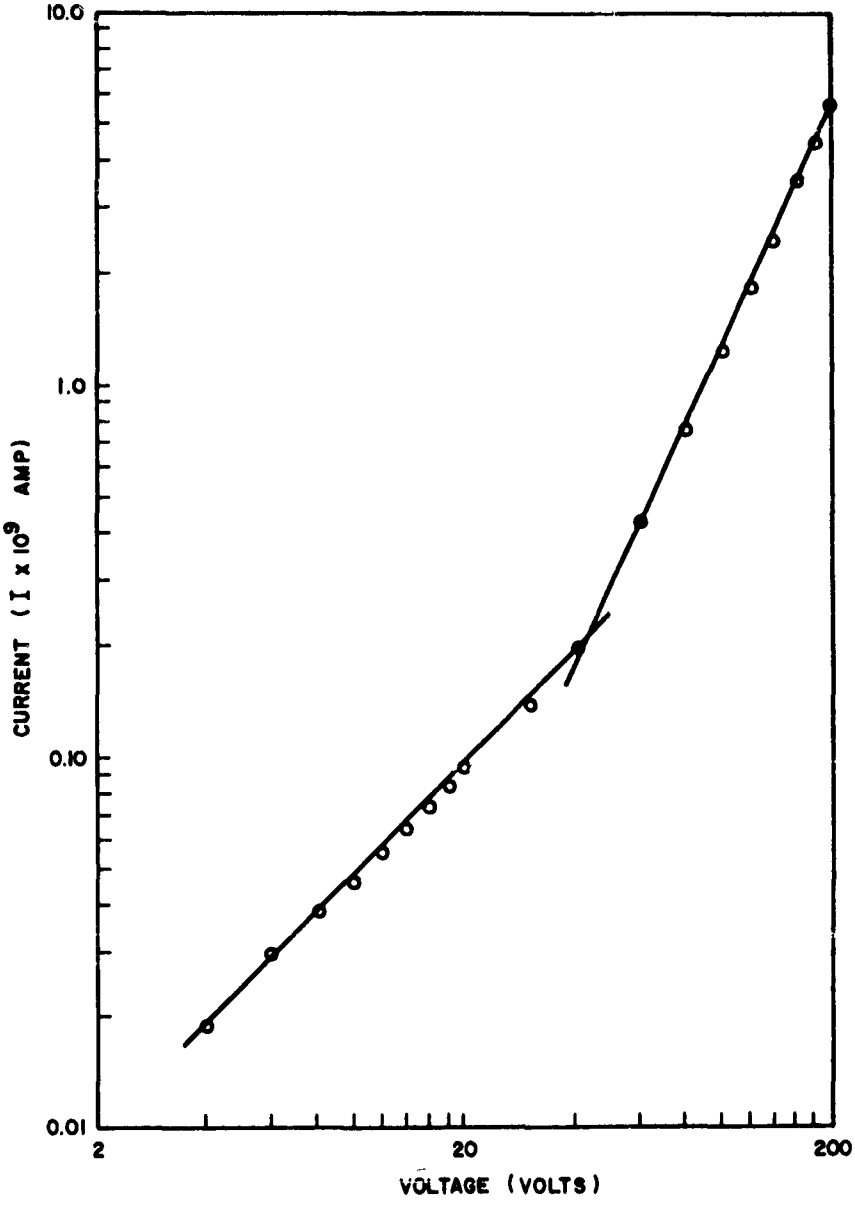

Current-voltage plot for crystal L-10, showing ohmic conduction below 44 volts and space-charge limited conduction at higher voltages.

$$J = \frac{10^{-13} V^2 \epsilon \mu A}{l^3} = 2 \times 10^{-9} \text{ amp}$$

for a voltage of 200 volts and a cross-sectional area A of 4×10^{-4} cm^2. The experimental value is 6×10^{-9} amp. The agreement is quite good. It might appear that the resistivity of the sample is too low. Actually it was necessary to illuminate the sample in order to get current readings within the limits set by the electrometer leakage currents. The incident radiation was 345 mμ.

Sample J-5 might have shown space charge limited currents if a high enough field had been applied.

2. Current Saturation

All other samples (illuminated or in dark conditions) displayed current-voltage characteristics of the type shown in Fig. 19. This is the type of I-V characteristic one would expect for a sample with the type of band structure envisioned to account for the anomalous photovoltaic effect, i.e., opposing barriers at each interface. Thus, the crystal should act like a number of pairs of diodes placed back to back. If one considers just two identical diodes back-to-back, the relation between the current (I) and the voltage (V) across both diodes is given by the expression,

$$I = I_o \tanh \alpha V \quad , \tag{33}$$

where I_o is the value of the current at saturation. α is e/2kT for two identical diodes. The results of plotting I/I_o versus $\tanh \beta V$ is presented in Fig. 20. I_o was estimated to be 0.050×10^{-11} amp and β was chosen as 0.0125. The points generally fall on straight lines but the slopes of the two lines are different. Here again, it must be emphasized that the junctions in the crystals are not all alike, as assumed above.

Fig. 19 Current-Voltage Curves for a Typical Crystal Showing Saturation Effect

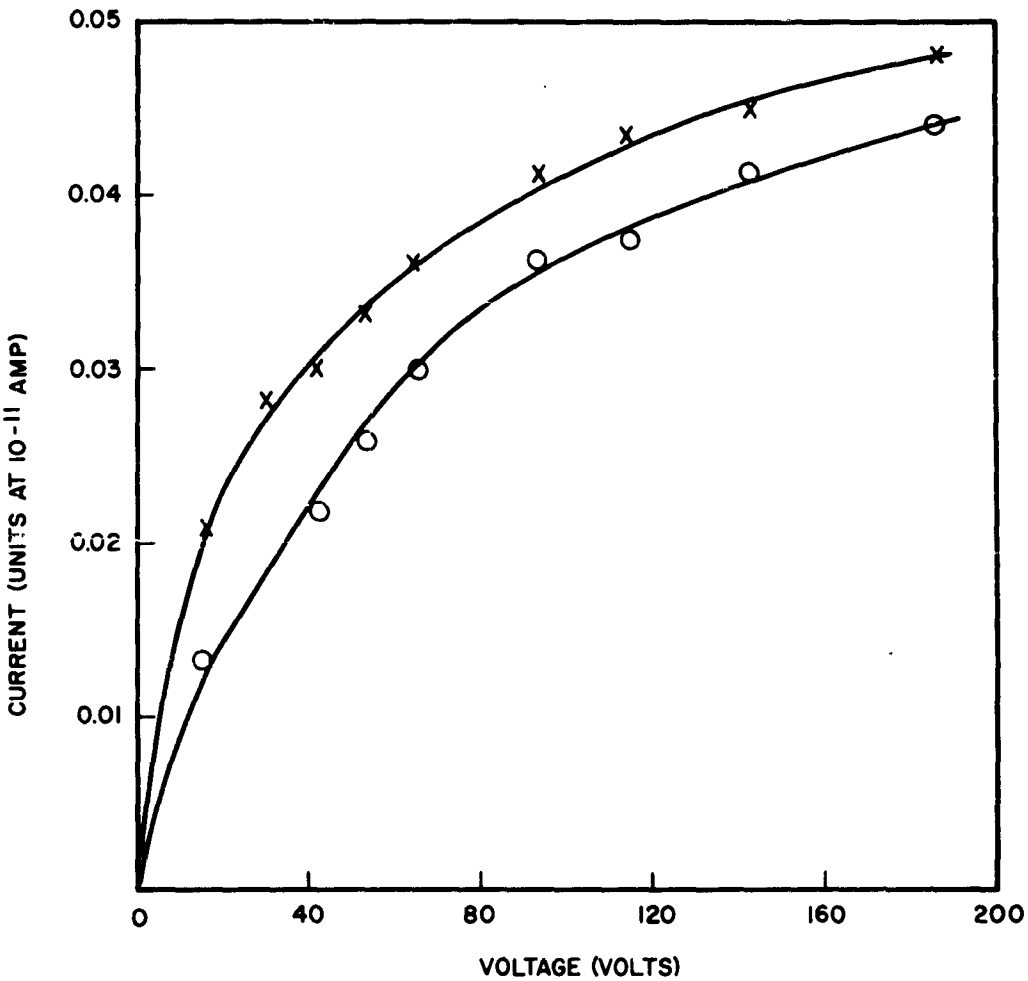

Current-voltage curves for a typical crystal showing saturation effect. The two curves are for different polarities.

Fig. 20 Current-Voltage Plot for Comparison Between Diode Theory and Experiment

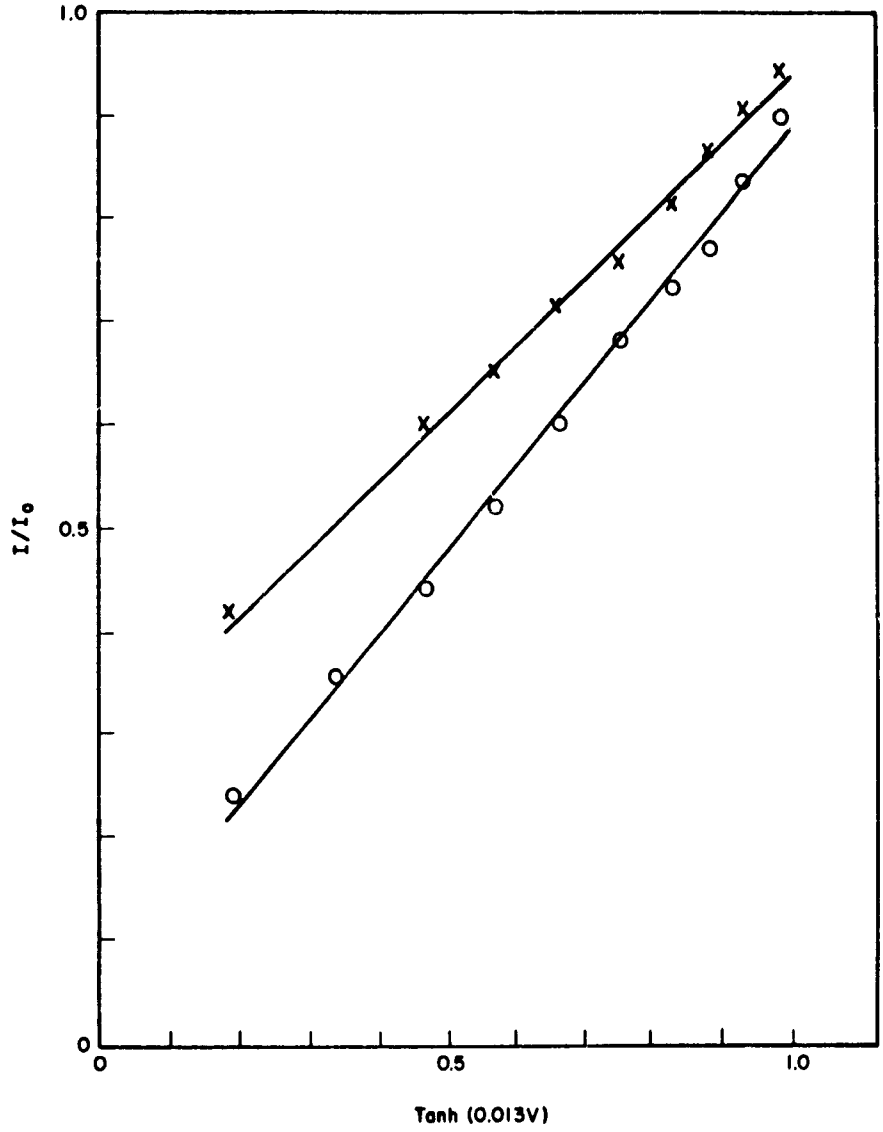

The data from Fig. 19 are replotted against tanh (0.013V). I_0 was estimated to be 0.05×10^{-11} amp for both curves.

Since the expression for the current is symmetric with respect to voltage, it is clear that one can predict the behavior of any number of diode pairs by simply replacing V in Equation (33) by V/N, where N is just the number of diode pairs. Conversely, one should be able to find the number of diode pairs from the experimental data. The constant β, chosen above to give a good fit between Equation (33) and the data, now becomes e/2NkT where N is the number of diode pairs. Using this argument, it was found that these crystals generally contain about 2,000 diode pairs per cm. According to the model of the APE, this means that there are about 4,000 layers/cm in the crystal. Merz,[4] using optical techniques, arrived at a figure of about 2,000 layers/cm.

VI. CONCLUSIONS

It was shown that earlier models failed to account for all the features of the APE. Specifically, both Tanc's model and Neumark's model could not account for the anomalously high voltages at both the positive and negative peaks, and the effect of polarized light on the spectral response curve. In addition, Tanc's scheme to add elemental voltages proved to be inadequate. The only objection to Hutson's model was that it was incomplete.

By extending Hutson's model and formulating the problem in terms of independent photovoltage generators in each segment of the crystal, one can account for all the features of the spectral response of the APE. Briefly, the present model correctly predicts the shape of the spectral response curve, the wavelengths at which the photovoltage changes polarity, and the general position of the photovoltage maxima. Furthermore, the model predicts the correct dependence of photocurrent on the polarization of incident light and the shift of λ_{OV} and λ_{OR} with temperature and light intensity.

The expression derived for the dependence of the photovoltage on an external applied stress, together with the results of the stress experiments on mixed crystals, verifies the assumption of the origin of the photovoltage, viz., that the photovoltages arise from piezoelectric fields set up by permanent internal strains formed during the growth process.

The experiment on single crystal hexagonal ZnS not only added strength to the proposed origin of the APE, but also successfully tied together the information on direction of crystal growth, pyroelectric effect, and the positive peak polarity. This experiment also verified the calculation of the photovoltage generated in a non-uniformly strained piezoelectric crystal.

In general then, the proposed model is quite successful; the main weakness of the model being the fact that the photovoltage depnds on the internal strain gradients, quantities which cannot be independently measured.

ACKNOWLEDGEMENT

I wish to thank Professor A. C. English for his support and interest in this work and for his many helpful suggestions.

APPENDIX

THEVENIN'S THEOREM FOR A PHOTOVOLTAIC GENERATOR

According to Tauc,[22] the field F is related to the current I, the conductivity σ, t_1, and t_2 the transfer coefficients for electrons and holes, and the chemical potentials for electrons and holes ζ_1 and ζ_2 by

$$F = \frac{I}{\sigma} - \frac{t_1}{e}\frac{d\zeta_1}{dx} + \frac{t_2}{e}\frac{d\zeta_2}{dx} .$$

To find the short-circuit current, it is necessary to solve the equation with the condition that

$$\oint F\,dx = 0 .$$

Thus,

$$\oint \frac{I}{\sigma}\,dx = \frac{1}{e}\oint\left(t_1\frac{d\zeta_1}{dx} - t_2\frac{d\zeta_2}{dx}\right)dx .$$

But since I is constant with respect to x, this equation can be rewritten as,

$$I_{sc} = \frac{\frac{1}{e}\oint\left(t_1\frac{d\zeta_1}{dx} - t_2\frac{d\zeta_2}{dx}\right)dx}{\oint\frac{dx}{\sigma}} ,$$

or replacing σ by ρ^{-1}, I_{sc} becomes

$$I_{sc} = \frac{1}{e}\oint\left(t_1\frac{d\zeta_1}{dx} - t_2\frac{d\zeta_2}{dx}\right)dx \Big/ \oint\rho\,dx .$$

Again referring to Tauc,[22] one finds that

$$\frac{1}{e}\oint\left(t_1\frac{d\zeta_1}{dx} - t_2\frac{d\zeta_2}{dx}\right)dx \equiv U_{OC} ,$$

where U_{OC} is the open-circuit voltage. Thus,

$$I_{sc} = \frac{U_{OC}}{\oint \rho\, dx} .$$

If it is assumed that the photogenerator extends from $x = a$ to $x = b$, has a unit cross-section, and that the circuit is completed by a resistanceless wire, then

$$I_{sc} = \frac{U_{OC}}{\int_a^b \rho\, dx} .$$

But,

$$\int_a^b \rho\, dx = R ,$$

where R is the total resistance between a and b in the light. Thus, I_{sc} can be written

$$I_{sc} = \frac{U_{OC}}{R} .$$

REFERENCES

1. S. G. Ellis, F. Herman, E. E. Loebner, W. J. Merz, C. W. Struck and J. G. White, Phys. Rev. 109, 1860 (1958).
2. A. Rose, J. Appl. Phys. 31, 1640 (1960).
3. H. A. Muser, Z. Physik 148, 308 (1957).
4. W. J. Merz, Helv. Phys. Acta 31, 625 (1958).
5. G. Cheroff and S. P. Keller, Phys. Rev. 111, 98 (1958).
6. E. I. Allen and J. L. Crenshaw, Am. J. Sci. 34, 341 (1912).
7. A. Kremheller, Sylvania Technologist 8, 11 (1955).
8. H. Samuelson, J. Appl. Phys. 32, 309 (1961).
9. D. C. Reynolds and L. C. Greene, J. Chem. Phys. 29, 1375 (1958).
10. F. A. Kröger, Physica 7, 1 (1940).
11. J. A. Beun and G. J. Goldsmith, Helv. Phys. Acta 33, 508 (1960).
12. W. W. Piper, Phys. Rev. 92, 23 (1953).
13. D. C. Reynolds and S. J. Czyzak, Phys. Rev. 79, 543 (1950).
14. W. W. Piper, P. D. Johnson and D. I. F. Marple, J. Phys. Chem. Solids 8, 457 (1959).
15. L. W. Strock and A. Brophy, Am. Mineralogist 40, 94 (1955).
16. L. W. Strock, Acta Cryst. 10, 840 (1957).
17. A. Lempicki, Phys. Rev. 113, 1204 (1959).
18. J. Tauc, J. Phys. Chem. Solids 17, 345 (1959).

19. A. D. Pogorelyi, Zhur. Fiz. Khim. 22, 731 (1948).

20. R. Nitsche, J. Phys. Chem. Solids 17, 163 (1960).

21. J. Tauc, Czechosl. J. Phys. 5, 178 (1955).

22. J. Tauc, Rev. Modern Phys. 29, 308 (1957).

23. G. Neumark, Phys. Rev. 125, 838 (1962).

24. A. R. Hutson, Bull. Am. Phys. Soc. 6, 110 (1961).

25. D. ter Haar, Elements of Statistical Mechanics (Rinehart & Co., New York, 1954), p. 229.

26. W. P. Mason, Piezoelectric Crystals and Their Applications to Ultrasonics (D. Van Nostrand Co., Inc., Princeton, New Jersey, 1950), p. 39.

27. W. Ehrenberg, Electric Conduction in Semiconductors and Metals (Oxford, Clarendon Press, 1958), p. 278.

28. G. Cheroff, Bull. Am. Phys. Soc. 6, 110 (1961).

29. P. Aigrain and M. Balkanski, Selected Constants Relative to Semiconductors (Pergamon Press, Oxford, 1961), p. 20.

30. Walter G. Cady, Piezoelectricity (McGraw-Hill Book Co., Inc., New York, 1946), p. 708.

31. A. G. Chynoweth, J. Appl. Phys. 27, 78 (1956).

32. Fred B. Seely and James O. Smith, Advanced Mechanics of Materials (Wiley, New York, 1952).

33. Albert Rose, Photoconductivity Conference 1954 (R. G. Breckenridge, Editor, Wiley, New York, 1956), p. 5.

34. A. R. Hutson, Phys. Rev. Letters 4, 505 (1960).

35. D. L. White, J. Appl. Phys. 33, 2547 (1962).

36. Clyde W. Moore, Silver Activation of Zinc Sulfide Single Crystals for Scintillation Counting, ASTIA 215-508 (also Masters Thesis for Air Force Institute of Technology, Wright-Patterson AFB, Dayton, Ohio) March 1959.

37. M. Aven and J. A. Parodi, J. Phys. Chem. Solids 13, 56 (1960).

38. M. A. Lampert, Phys. Rev. 103, 1648 (1956).

39. R. H. Bube, Photoconductivity of Solids (Wiley, New York, 1960), p. 120.